Table 2. Clinical Characteristics of the Groups Divided by Serum L-PGDS Level

	Quartile 1	Quartile 2	Quartile 3	Quartile 4	*p*
Women					
Number	86	86	86	84	
Serum L-PGDS, mg/L (range)	0.39 (0.25–0.44)	0.48 (0.44–0.52)	0.56 (0.52–0.61)	0.72 (0.61–1.21)	<0.001
Age, years	54.3	57.8	61.1	65.3	<0.001
Habitual smoking, %	2.3	8.1	16.3	14.5	0.010
Body mass index, kg/m^2	23.0	23.9	23.9	23.9	n.s.
Systolic BP, mmHg	122.8	130.3	131.6	138.5	<0.001
Diastolic BP, mmHg	73.6	76.9	77.2	77.2	n.s.
HDL-cholesterol, mmol/L	1.7	1.7	1.7	1.6	n.s.
LDL-cholesterol, mmol/L	3.4	3.5	3.6	3.5	n.s.
FPG, mmol/L	5.3	5.2	5.0	5.1	n.s.
Serum creatinine, μmol/L	60.8	61.3	62.1	71.7	<0.001
Men					
Number	39	40	39	40	
Serum L-PGDS, mg/L (range)	0.43 (0.25–0.49)	0.54 (0.50–0.58)	0.62 (0.58–0.67)	0.79 (0.67–1.27)	<0.001
Age, years	56.4	58.2	63.4	69.1	<0.001
Habitual smoking, %	28.2	30.0	23.1	20.0	n.s.
Body mass index, kg/m^2	24.1	23.3	24.6	23.9	n.s.
Systolic BP, mmHg	132.3	130.5	129.4	142.2	0.039
Diastolic BP, mmHg	78.2	77.4	78.6	84.8	0.047
HDL-cholesterol, mmol/L	1.6	1.6	1.4	1.4	0.032
LDL-cholesterol, mmol/L	3.4	3.5	3.4	3.2	n.s.
FPG, mmol/L	5.9	5.5	5.5	5.9	n.s.
Serum creatinine, μmol/L	77.8	80.5	85.4	93.6	<0.001

Values are the means or frequency. *p* values refer to ANOVA. n.s., not significant; L-PGDS, lipocalin-type prostaglandin D synthase; other abbreviations as shown in Table 1.

risk factors, age-adjusted L-PGDS levels were significantly elevated in subjects with two or more risk factors, for both genders, compared to those without risk factors (Fig. 3).

Association of Serum L-PGDS with Surrogate Atherosclerotic Indices

Next, we examined the association between serum L-PGDS and subclinical atherosclerotic indices. The values of C-IMT$_{max}$ and ba-PWV were 1.20±0.03 mm (men: 1.40±0.07; women: 1.11±0.03) and 15.7±0.2 m/s (men: 16.4±0.3; women: 15.3±0.2), respectively. In a simple regression analysis, C-IMT$_{max}$ showed a significant positive correlation with age, serum creatinine and LDL cholesterol. The values of ba-PWV were also associated with age, BP, FPG, serum creatinine and serum L-PGDS. The serum L-PGDS level (log scale) was significantly associated with both C-IMT$_{max}$ (women: r=0.125, p=0.021; men: r=0.108, p=0.175; all: r=0.150, p<0.001) and ba-PWV (women: r=0.328, p<0.001; men: r=0.360, p<0.001; all: r=0.354, p<0.001) in a linear regression model. When the subjects were divided into four groups according to the L-PGDS levels (Table 2), age-adjusted values of C-IMT$_{max}$ and ba-PWV were significantly higher in subjects in quartile 3 and quartile 4 compared to those in quartile 1, in both genders (Fig. 4). In a multiple regression analysis including traditional atherosclerotic risk factors, age and hypertension were independently associated with ba-PWV (Table 3). The serum L-PGDS level was also detected as an independent determinant for ba-PWV (β=0.130, p<0.001). For C-IMT$_{max}$, age, obesity, dyslipidemia and serum creatinine were detected as independent factors. Serum L-PGDS tended to associate with C-IMT$_{max}$, but this was not statistically significant (β=0.084, p=0.075). Finally, we determined the appropriate cut-off values of serum L-PGDS in relation to each atherosclerotic index using ROC curve analysis. The optimal cut-off points of the regression model for increased ba-PWV (≥14.0 m/s) and C-IMT$_{max}$ (≥1.0 mm) were 0.57 and 0.58 mg/L in men, and 0.53 and 0.53 mg/L in women, respectively.

Discussion

In the present study, the serum L-PGDS concentration measured by ELISA was comparable to those obtained in healthy subjects in previous studies (*16, 20, 21*). Serum L-PGDS levels increased with aging and showed a significant difference between genders. Furthermore, serum L-PGDS levels increased with increasing numbers of the traditional athero-

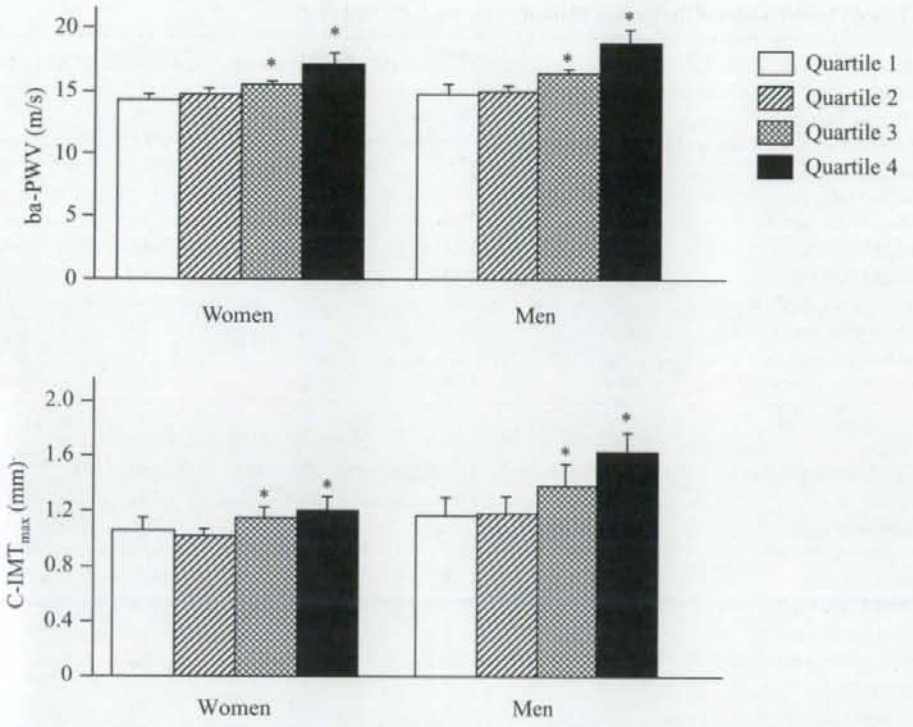

Fig. 4. *Comparison of the age-adjusted values of the atherosclerotic indices (top, ba-PWV; bottom, C-IMT$_{max}$) among groups divided according to the serum L-PGDS levels. *$p<0.05$ vs. quartile 1. ba-PWV, brachial-ankle pulse wave velocity; C-IMT$_{max}$, maximum intima-media complex thickness of the carotid artery.*

Table 3. Multiple Regression Analyses for Vascular Properties

Risk factors	C-IMT$_{max}$		ba-PWV	
	β	p	β	p
Men	0.093	0.064	0.058	0.180
Age	0.458	<0.001	0.463	<0.001
Habitual smoking	0.074	0.069	−0.008	0.815
Obesity	0.093	0.021	−0.029	0.408
Hypertension	0.017	0.687	0.251	<0.001
Dyslipidemia	0.083	0.036	0.011	0.741
Diabetes	0.003	0.942	0.028	0.417
Serum creatinine	0.105	0.049	0.013	0.771
$\log_{10}$ L-PGDS	0.084	0.075	0.130	<0.001

C-IMT$_{max}$, maximum intima-media complex thickness of the carotid artery; ba-PWV, brachial-ankle pulse wave velocity; L-PGDS, lipocalin-type prostaglandin D synthase.

sclerotic risk factors and were associated with the atherosclerotic changes of the vascular wall (*i.e.*, C-IMT$_{max}$ and ba-PWV). When we determined the cut-off values of L-PGDS for the atherosclerotic indices calculated by ROC curve analysis, these were approximately equal to the median values (men=0.58 mg/L, women=0.52 mg/L). As shown in Fig. 4, age-adjusted values of the atherosclerotic markers increased from quartile 3 (=median values) in men and women, suggesting that these cut-off values are reasonable and useful to predict the atherosclerotic changes of the vascular wall. How-

ever, because this study was cross-sectional in design, further investigation is required to confirm whether these are actually appropriate values.

Although it remains largely unknown how serum L-PGDS levels are regulated, a possible source of L-PGDS is the vascular endothelium in normal vessels. We previously reported that fluid shear stress induced L-PGDS expression in vascular endothelial cells and subsequently released downstream PGs, PGD_2 and 15d-PGJ_2, into the culture medium (*22*). L-PGDS expression in endothelial cells depends on the strength of the shear stress, and therefore the hemodynamic changes accompanying elevated BP and the morphological and functional changes of the vascular wall could alter the serum L-PGDS levels. The increase in serum L-PGDS in hypertensives, in our results as well as in the previous report (*16*), supports this hypothesis. Another possible source is the intimal de-differentiated VSMCs in the atherosclerotic region because the expression of L-PGDS was also found in the atherosclerotic intima (*1*). In our results, the serum L-PGDS level showed a strong correlation with aging and hypertension, which are the most powerful inducers of the atherosclerotic change of the vascular wall, and increased as the number of risk factors increased. Moreover, serum L-PGDS levels were associated with C-IMT_{max}, which reflects the degree of intimal thickening. Therefore, it seemed probable that L-PGDS is induced by the neointimal VSMCs in the atherosclerotic lesion of the vascular wall.

We found no significant association between serum L-PGDS and diabetes mellitus. Other researchers have reported that plasma concentrations of L-PGDS were slightly higher in patients with diabetes mellitus than in control subjects, although the differences did not reach significance (*20*). However, a recent report suggested that a high concentration of glucose induces L-PGDS expression and that exogenous L-PGDS inhibits cell proliferation and migration in vascular smooth muscle cells explanted from Goto-Kakizaki rats, a model of type II diabetes (*2*). Furthermore, one of the downstream PGs of L-PGDS, 15d-PGJ_2, is well known as a strong endogenous ligand of PPAR-γ, which is closely associated with insulin sensitivity. Since we excluded the severe diabetic subjects, further detailed study in a large population is required to clarify this issue.

Another interesting finding is the inverse correlation between serum L-PGDS and HDL-cholesterol. Considering the significant association between atherosclerotic risk factors and serum L-PGDS, a direct correlation might seem natural because decreased HDL cholesterol is one of the risk factors of atherosclerosis. However, we recently found an association between the human L-PGDS gene polymorphism and HDL-cholesterol levels (*23*). In subjects with the A/A genotype of 4111A>C, serum levels of HDL cholesterol were significantly higher than in those with the A/C and C/C genotypes. Although further studies are required, L-PGDS may play a role in lipid transport because L-PGDS belongs to the lipocalin superfamily, a group of proteins that bind and transport small lipophilic molecules.

There are several limitations of this study. Because its design is cross-sectional, we could not confirm whether the increase in serum L-PGDS in subjects with mild atherosclerosis is a cause or a consequence at this stage. Additionally, the L-PGDS concentration might not represent its enzymatic activity. To determine the L-PGDS activity, measurement of the serum levels of downstream PGs may be useful; however, PGD_2 and PGJ_2 series are unstable substances and measuring their serum levels is quite difficult. To determine the precise role of L-PGDS in the pathogenesis of atherosclerosis, further clinical investigations using prospective designs and basic research using animal models such as L-PGDS knockout mice are required.

In conclusion, our results showed that serum L-PGDS levels increase with the increasing number of traditional atherosclerotic risk factors in a relatively large asymptomatic population. For the first time, we provided evidence that the increase in serum L-PGDS is associated with the atherosclerotic changes of the vascular wall. L-PGDS may be involved in the development of atherosclerosis, although further study is necessary to clarify its pathophysiologic role.

Acknowledgements

We thank all the staff members who supported the medical examination. We are also grateful to Kana Oie for her secretarial assistance.

References

1. Eguchi Y, Eguchi N, Oda H, *et al*: Expression of lipocalin-type prostaglandin D synthase (beta-trace) in human heart and its accumulation in the coronary circulation of angina patients. *Proc Natl Acad Sci U S A* 1997; **94**: 14689–14694.
2. Taba Y, Sasaguri T, Miyagi M, *et al*: Fluid shear stress induces lipocalin-type prostaglandin D_2 synthase expression in vascular endothelial cells. *Circ Res* 2000; **86**: 967–973.
3. Ragolia L, Palaia T, Koutrouby TB, Maesaka JK: Inhibition of cell cycle progression and migration of vascular smooth muscle cells by prostaglandin D2 synthase: resistance in diabetic Goto-Kakizaki rats. *Am J Physiol Cell Physiol* 2004; **287**: C1273–C1281.
4. Cipollone F, Fazia M, Iezzi A, *et al*: Balance between PGD synthase and PGE synthase is a major determinant of atherosclerotic plaque instability in humans. *Arterioscler Thromb Vasc Biol* 2004; **24**: 1259–1265.
5. Ragolia L, Palaia T, Hall CE, Maesaka JK, Eguchi N, Urade Y: Accelerated glucose intolerance, nephropathy, and atherosclerosis in prostaglandin D2 synthase knock-out mice. *J Biol Chem* 2005; **280**: 29946–29955.
6. Bushfield M, McNicol A, MacIntyre DE: Inhibition of platelet-activating-factor–induced human platelet activation by prostaglandin D2. Differential sensitivity of platelet transduction processes and functional responses to inhibition by cyclic AMP. *Biochem J* 1985; **232**: 267–271.
7. Negishi M, Sugimoto Y, Ichikawa A: Prostanoid receptors and their biological actions. *Prog Lipid Res* 1993; **32**:

417–434.

8. Nagoshi H, Uehara Y, Kanai F, *et al*: Prostaglandin D2 inhibits inducible nitric oxide synthase expression in rat vascular smooth muscle cells. *Circ Res* 1998; **82**: 204–209.
9. Negoro H, Soo Shin W, Hakamada-Taguchi R, *et al*: Endogenous prostaglandin D2 synthesis reduces an increase in plasminogen activator inhibitor-1 following interleukin stimulation in bovine endothelial cells. *J Hypertens* 2002; **20**: 1347–1354.
10. Ricote M, Li AC, Willson TM, Kelly CJ, Glass CK: The peroxisome proliferator–activated receptor-gamma is a negative regulator of macrophage activation. *Nature* 1998; **391**: 79–82.
11. Jiang C, Ting AT, Seed B: PPAR-γ agonists inhibit production of monocyte inflammatory cytokines. *Nature* 1998; **391**: 82–86.
12. Marx N, Sukhova G, Murphy C, Libby P, Plutzky J: Macrophages in human atheroma contain PPARγ: differentiation-dependent peroxisomal proliferator–activated receptor γ (PPARγ) expression and reduction of MMP-9 activity through PPARγ activation in mononuclear phagocytes *in vitro*. *Am J Pathol* 1998; **153**: 17–23.
13. Sasaguri T, Masuda J, Shimokado K, *et al*: Prostaglandins A and J arrest the cell cycle of cultured vascular smooth muscle cells without suppression of c-myc expression. *Exp Cell Res* 1992; **200**: 351–357.
14. Miwa Y, Sasaguri T, Inoue H, Taba Y, Ishida A, Abumiya T: 15-Deoxy-$\Delta^{12,14}$-prostaglandin J_2 induces G_1 arrest and differentiation marker expression in vascular smooth muscle cells. *Mol Pharmacol* 2000; **58**: 837–844.
15. Miwa Y, Takahashi-Yanaga F, Morimoto S, Sasaguri T: Involvement of clusterin in 15-deoxy-$\Delta^{12,14}$-prostaglandin J_2–induced vascular smooth muscle cell differentiation. *Biochem Biophys Res Commun* 2004; **319**: 163–168.
16. Hirawa N, Uehara Y, Yamakado M, *et al*: Lipocalin-type prostaglandin D synthase in essential hypertension. *Hypertension* 2002; **39**: 449–454.
17. Inoue T, Takayanagi K, Morooka S, *et al*: Serum prostaglandin D synthase level after coronary angioplasty may predict occurrence of restenosis. *Thromb Haemost* 2001; **85**: 165–170.
18. Oda H, Shiina Y, Seiki K, Sato N, Eguchi N, Urade Y: Development and evaluation of a practical ELISA for human urinary lipocalin-type prostaglandin D synthase. *Clin Chem* 2002; **48**: 1445–1453.
19. Nakamura U, Iwase M, Nohara S, Kanai H, Ichikawa K, Iida M: Usefulness of brachial-ankle pulse wave velocity measurement: correlation with abdominal aortic calcification. *Hypertens Res* 2003; **26**: 163–167.
20. Hirawa N, Uehara Y, Ikeda T, *et al*: Urinary prostaglandin D synthase (beta-trace) excretion increases in the early stage of diabetes mellitus. *Nephron* 2001; **87**: 321–327.
21. Hamano K, Totsuka Y, Ajima M, *et al*: Blood sugar control reverses the increase in urinary excretion of prostaglandin D synthase in diabetic patients. *Nephron* 2002; **92**: 77–85.
22. Taba Y, Miyagi M, Miwa Y, *et al*: 15-Deoxy-$\Delta^{12,14}$-prostaglandin J_2 and laminar fluid shear stress stabilize c-IAP1 in vascular endothelial cells. *Am J Physiol Heart Circ Physiol* 2003; **285**: H38–H46.
23. Miwa Y, Takiuchi S, Kamide K, *et al*: Identification of gene polymorphism in lipocalin-type prostaglandin D synthase and its association with carotid atherosclerosis in Japanese hypertensive patients. *Biochem Biophys Res Commun* 2004; **322**: 428–433.

Biochemical and Biophysical Research Communications 377 (2008) 1185–1190

Contents lists available at ScienceDirect

Biochemical and Biophysical Research Communications

journal homepage: www.elsevier.com/locate/ybbrc

Celecoxib-induced degradation of T-cell factors-1 and -4 in human colon cancer cells

Fumi Takahashi-Yanaga [a,*], Tatsuya Yoshihara [a], Kentaro Jingushi [a], Yoshikazu Miwa [a], Sachio Morimoto [a], Masato Hirata [b], Toshiyuki Sasaguri [a]

[a] Department of Clinical Pharmacology, Faculty of Medical Sciences, Kyushu University, Fukuoka, 812-8582, Japan
[b] Department of Molecular and Cellular Biochemistry, Faculty of Dental Sciences, Kyushu University, Fukuoka, 812-8582, Japan

ARTICLE INFO

Article history:
Received 9 October 2008
Available online 5 November 2008

Keywords:
Celecoxib
Wnt/β-catenin signaling pathway
T-cell factor (TCF)
Colon cancer cell

ABSTRACT

We examined the effect of celecoxib on the expression of T-cell factors (TCFs) to clarify the mechanism by which celecoxib suppress β-catenin/TCF-dependent transcriptional activity without reducing the level of β-catenin protein, using HCT-116 cells. Celecoxib suppressed the expression of TCF-1 and TCF-4 in a time-dependent manner. Pretreatment of cells with the proteasome inhibitor MG132 inhibited the loss of TCF-1 and TCF-4 induced by celecoxib, suggesting that celecoxib induced the proteasome-dependent degradation of TCF-1 and TCF-4. β-Catenin/TCF-dependent transcriptional activity was significantly decreased after the treatment with celecoxib for 6 h and the pretreatment of the cells with MG132 attenuated the effect of celecoxib. Further, celecoxib also suppressed the expression of TCF-1 and TCF-4 in another colon cancer cell line, DLD-1. Our results suggest that TCF-1 and TCF-4 degradation may involve the inhibition of the Wnt/β-catenin signaling pathway induced by celecoxib.

Most colorectal cancers have somatic mutations in adenomatous polyposis coli (APC) or β-catenin, which are members of the Wnt/β-catenin signaling pathway [1–4]. Although this pathway is essential to regulate gene transcription during embryo development, it is probably present in intestinal crypts throughout adult life, maintaining the balance between cell proliferation and differentiation [5,6]. The activity of this signaling pathway is determined by the amount of β-catenin in the cytoplasm. Normally, the cytoplasmic β-catenin level is kept low through continuous ubiquitin-proteasome-mediated degradation of β-catenin, which is regulated by a multiprotein complex (β-catenin destruction complex) containing axin, APC, glycogen synthase kinase-3β, and casein kinase 1α [7,8]. Mutations in APC and β-catenin retard β-catenin degradation by this system leading to accumulation of β-catenin in the cytoplasm and its translocation into the nucleus, resulting in the up-regulation of Wnt/β-catenin signaling pathway target genes together with T-cell factor (TCF). It has been reported that constant activation of this signaling pathway can lead to cancer.

Numerous experimental and epidemiological studies in humans suggest that aspirin and other nonsteroidal anti-inflammatory drugs (NSAIDs) have chemopreventive activity against colon cancer [9–11]. Several randomized trials have shown the growth inhibition of polyps and a decrease in the number of existing polyps in patients with familial adenomatous polyposis (FAP) who received sulindac or celecoxib [12,13]. Two randomized placebo-controlled studies have shown that aspirin reduced the risk of colorectal adenomas among individuals with previous colorectal cancer and adenoma, excluding FAP patients [14,15]. The possible cellular mechanisms underlying these chemopreventive effects of NSAIDs have been thought to be the induction of apoptosis, cell-cycle arrest and the inhibition of angiogenesis [10,11]. Moreover, NSAIDs have been reported to inhibit the Akt [16,17] and the Wnt/β-catenin signaling pathways [18–21].

Celecoxib is the only NSAID approved by the Food and Drug Administration for the treatment of FAP patients. However, the molecular mechanism responsible for the chemopreventive effect of celecoxib is not entirely understood. Although this compound was developed as a selective cyclooxygenase-2 (COX-2) inhibitor, additional pharmacological activities have emerged outside of its cox-2 inhibition. Celecoxib has potency to inhibit COX-2 activity at nanomolar range, however, it requires micromolar range to inhibit cellular proliferation and survival [22,23]. We previously reported that celecoxib inhibited β-catenin/TCF-dependent transcriptional activity without affecting the amount of β-catenin protein using HCT-116 cells which lack COX-2 expression, suggesting that this effect was COX-2-independent [24]. Recently, it has been reported that the TCF transcription factors TCF-4 and LEF-1 are ubiquitylated and degraded via the proteasome system [25]. Therefore, we examined the effect of celecoxib on TCF-1 and TCF-4 expression levels to identify the mechanism by which celecoxib reduces β-catenin/TCF-dependent transcriptional activity.

* Corresponding author. Fax: +81 92 642 6084.
E-mail address: yanaga@clipharm.med.kyushu-u.ac.jp (F. Takahashi-Yanaga).

0006-291X/$ - see front matter © 2008 Elsevier Inc. All rights reserved.
doi:10.1016/j.bbrc.2008.10.115

Our results suggested that celecoxib induces TCF-1 and TCF-4 degradation via the proteasome system without affecting β-catenin protein amount in the colon cancer cell lines HCT-116 and DLD-1. To our knowledge, this is the first report to show celecoxib induce the degradation of TCF family members.

Materials and methods

Chemicals and antibodies. TOPflash (a TCF reporter plasmid) and FOPflash (a negative control for TOPflash) were purchased from Upstate Biotechnology. The monoclonal anti-GAPDH antibody was from Abcam. The monoclonal anti-TCF-4 antibody (6H5-3) was from Cell Signaling Technology (Danvers, MA). The polyclonal anti-TCF-1 (H-18) antibody was from Santa Cruz Biotechnology. The monoclonal anti-β-catenin antibody was from BD Biosciences. MG132 was from Peptide Institute (Osaka, Japan). Celecoxib was kindly provided by Pfizer.

Cell culture. HCT-116 cells, a human colon cancer cell line expressing wild-type APC and mutated β-catenin but lacking COX-2 [1,26–28], and DLD-1 cells, a human colon cancer cell line expressing mutated APC and wild-type β-catenin but lacking COX-2 [2,28,29], were grown in Dulbecco's modified Eagle's medium (Sigma) supplemented with 10% fetal bovine serum (FBS), 100 U/ml of penicillin G, and 0.1 μg/ml of streptomycin.

Immunoblotting. Immunoblotting analysis was performed as described previously [30]. Briefly, samples (10 μg/lane) were separated by 12% SDS–polyacrylamide gel electrophoresis (SDS–PAGE) and transferred to a polyvinylidene difluoride membrane using a semi-dry transfer system (1 h, 12 V). After blocking with 5% skim milk for 1 h, the membrane was probed with a first antibody. The membrane was washed three times and incubated with horseradish peroxidase-conjugated anti-rabbit or anti-mouse IgG (Cell Signaling Technology) for 1 h. Immunoreactive proteins on the membrane were visualized by treatment with a detection reagent (LumiGLO, Cell Signaling Technology). An optical densitometric scan was performed using Science Lab 99 Image Gauge Software (Fuji Photo Film).

Luciferase reporter assay. Cells were transfected with luciferase reporter plasmid (TOPflash or FOPflash) and pRL-SV40, a *Renilla* luciferase expression plasmid for the control of transfection efficiency, using Lipofectamine Plus reagent (Invitrogen). Cells were cultured for 24 h after transfection and stimulated with celecoxib (100 μM) for the period indicated. To evaluate the effect of MG132 on celecoxib action, transfected cells were treated with 10 μM of MG132 for 1 h and then stimulated with celecoxib for 6 h. Luciferase activity was determined with a luminometer (Lumat LB 9507, Berthold Technologies) and normalized with respect to *Renilla* luciferase activity.

Statistical analysis. The results are expressed as means ± SE. Statistical analysis of differences between two means was performed using the Student's *t*-test.

Results

Celecoxib induces TCF-1 and TCF-4 protein degradation in HCT-116 cells

We first examined whether celecoxib affects TCF-1 and TCF-4 expression in the human colon cancer cell line HCT-116. Cells were incubated with or without celecoxib for the indicated period, and the expression levels of TCF-1 and TCF-4 were examined by immunoblotting. Two bands were detected by antibody against TCF-1 and upper band was interpreted as non-specific bands from their molecular weight. The protein amounts of both TCF-1 and TCF-4 gradually increased with incubation period in control cells. On the other hand, the both protein amounts in 100 μM celecoxib-treated cells were significantly reduced after a 3-h treatment (Fig. 1A). Although we previously reported that celecoxib induced apoptosis in human colon cancer cell lines, degradation of TCF transcription factors induced by celecoxib was unlikely to be caused by cytotoxicity, because caspase-3 activity was not increased after 6-h treatment [24]. As shown in Fig. 1B, celecoxib decreased in the levels of TCF-1 and TCF-4 at 100 μM whereas it did not have significant effect until 50 μM. Thus, celecoxib reduced the protein levels of both TCF-1 and TCF-4 in a time-dependent manner at a concentration of 100 μM. We next examined the effect of the proteasome inhibitor MG132 on celecoxib-induced reduction of TCF-1 and TCF-4. Cells were treated with or without 10 μM MG132 for 1 h and stimulated with or without 100 μM celecoxib for 6 h. As shown in Fig. 2, pretreatment with MG132 significantly attenuated the effect of celecoxib, indicating that celecoxib accelerated the proteasome-dependent degradation of TCF-1 and TCF-4 in HCT-116 cells.

Celecoxib reduces β-catenin/TCF-dependent transcriptional activity

Subsequently, the effect of celecoxib on the expression level of β-catenin was examined using HCT-116 cells, which has been reported to express stable β-catenin due to the mutation [1,26–28]. As shown in Fig. 3A, celecoxib did not affect the amount of β-catenin protein in the first 24 h of incubation and this result is well correlated with our previous report [24]. The effect of celecoxib on β-catenin/TCF-dependent transcriptional activity was examined using TCF reporter plasmid TOPflash and its negative control FOPflash. Celecoxib reduced TOPflash activity in a time-dependent manner without affecting FOPflash activity (Fig. 3B). Although we found that celecoxib significantly reduced the protein levels of TCF-1 and TCF-4 after a 3-h incubation, TOPFlash activity was not significantly affected after a 3-h incubation. Celecoxib gradually reduced the TOPFlash activity after a 6-h treatment. These results suggested that celecoxib might reduce β-catenin/TCF-dependent transcriptional activity due to the degradation of TCF transcription factors, and that this effect was independent of the β-catenin protein level. To clarify this point, we next examined the effect of celecoxib on β-catenin/TCF-dependent transcriptional activity using proteasome inhibitor MG132. For this purpose, transfected HCT-116 cells were pretreated with 10 μM of MG132 for 1 h and stimulated with celecoxib for 12 h. However, all most all cells treated with MG132 were died at the end of incubation period due to the cytotoxic effect of proteasome inhibitor (data not shown). Therefore, incubation period was shortened and the effect of celecoxib was evaluated after a 6-h treatment. As shown in Fig. 3C, although celecoxib significantly inhibited TOPFlash activity after a 6-h treatment, pretreatment with MG132 attenuated the effect of celecoxib. These results clearly indicated that the reduction of the β-catenin/TCF-dependent transcriptional activity was due to the degradation of TCF transcription factors.

Effect of celecoxib on TCF-1 and TCF-4 protein amounts in another colon cancer cell line, DLD-1

The effect of celecoxib was also examined using the human colon cancer cell line DLD-1, which has mutation in APC and β-catenin degradation system is retarded [2,28]. As we previously reported that the same concentrations of celecoxib used in HCT-116 cells did not have significant effects on this cell line, we used a higher concentration of celecoxib (200 μM) for this experiment. As shown in Fig. 4A, 200 μM celecoxib greatly reduced the amounts of TCF-1 and TCF-4 proteins in a time-dependent manner, but had no significant effect on the expression of β-catenin in DLD-1 cells. Moreover, pretreatment with proteasome inhibitor MG132,

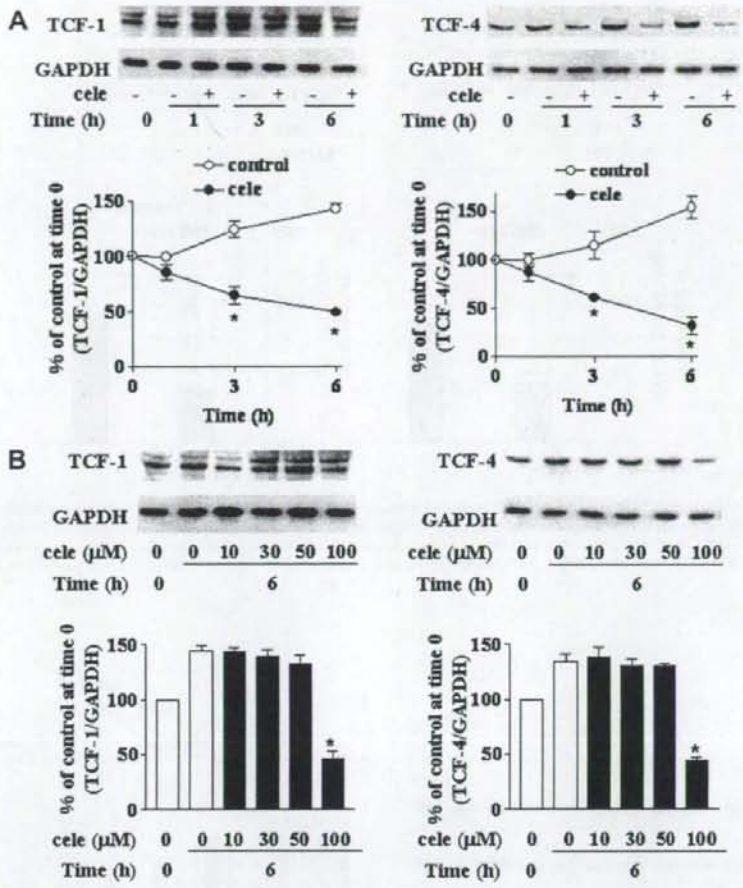

Fig. 1. The effect of celecoxib on the expression of TCF-1 and TCF-4. (A) Time course. HCT-116 cells were incubated with or without celecoxib (100 μM) for the period indicated. Protein samples were collected and separated by 12% SDS–PAGE and immunoblotted with the anti-TCF-1 antibody (left) or anti-TCF-4 antibody (right). (B) Dose dependency. HCT-116 cells were incubated with or without various amounts of celecoxib for 6 h. Protein samples were collected and separated by 12% SDS–PAGE and immunoblotted with the anti-TCF-1 antibody (left) or anti-TCF-4 antibody (right). The membrane was reprobed with anti-GAPDH antibody. The levels of protein bands were quantified and normalized to those of GAPDH. The results are shown as a percentage of the control level at time 0. Values are the means ± SE of three independent experiments. $^{*}p < 0.01$ vs. control (Student's *t*-test), cele: celecoxib.

inhibited the effect of celecoxib, indicating that celecoxib accelerated the proteasome-dependent degradation of TCF-1 and TCF-4 in DLD-1 cells (Fig. 4B). Taken together, these results indicated that celecoxib induced proteasome-dependent degradation of TCF-1 and TCF-4 in colon cancer cell lines, while the sensitivity to celecoxib is different among cell lines.

Discussion

In this study, we showed that celecoxib induced the degradation of TCF-1 and TCF-4 in human colon cancer cell lines. Constitutive activation of the Wnt/β-catenin signaling pathway could trigger the formation of colon cancers. Activation of this pathway is due to genetic mutations that stabilize the β-catenin protein, allowing it to accumulate in the nucleus and form complexes with TCF transcription factors to activate the transcription of target genes. It has been proposed that abnormal expression levels or patterns of the target genes such as MYC, CCND1 and MMP7 have a role in tumor progression [1–4]. Therefore, anticancer drugs that suppress the transcriptional activity of the Wnt/β-catenin signaling pathway could be of important therapeutic value against colon cancers. Although one well known mechanism for suppressing the transcriptional activity of Wnt/β-catenin signaling pathway is β-catenin degradation, it is quite difficult to induce the degradation of β-catenin in most colon cancer cells due to mutations in β-catenin or components of the β-catenin destruction complex (including axin and APC), as described above. However, as shown in this study, celecoxib induced degradation of TCF transcription factors and inhibited the transcriptional activity of the Wnt/β-catenin signaling pathway. This might represent a new mechanism for inhibiting the transcriptional activity of the Wnt/β-catenin signaling pathway.

COX-2 is the key enzyme in the conversion of arachidonic acid to prostaglandins which promote cell proliferation, angiogenesis and inhibit the induction of apoptosis; therefore, the chemopreventive effect of NSAIDs is thought to be attributed to their COX-2 inhibitory activity. However, some studies have suggested that celecoxib has anticarcinogenic effects in cells which do not express COX-2 and COX-2-deficient tumors in a nude mice model [26,27]. In fact, the HCT-116 cells and DLD-1 cells used in this experiment

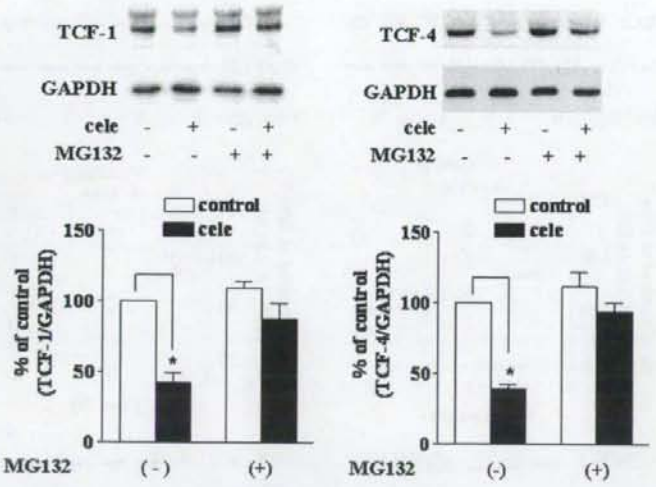

Fig. 2. Effect of the proteasome inhibitor MG132. HCT-116 cells were incubated with or without 10 μM MG132 for 1 h and stimulated with or without celecoxib (100 μM) for 6 h. Protein samples were collected and separated by 12% SDS–PAGE and immunoblotted with the anti-TCF-1 antibody (left) or anti-TCF-4 antibody (right). The membrane was reprobed with the anti-GAPDH antibody. The levels of protein bands were quantified and normalized to those of GAPDH. The results are shown as a percentage of the control level. Values are the means ± SE of three independent experiments performed in duplicate. $^{*}p < 0.01$ vs. control (Student's *t*-test), cele: celecoxib.

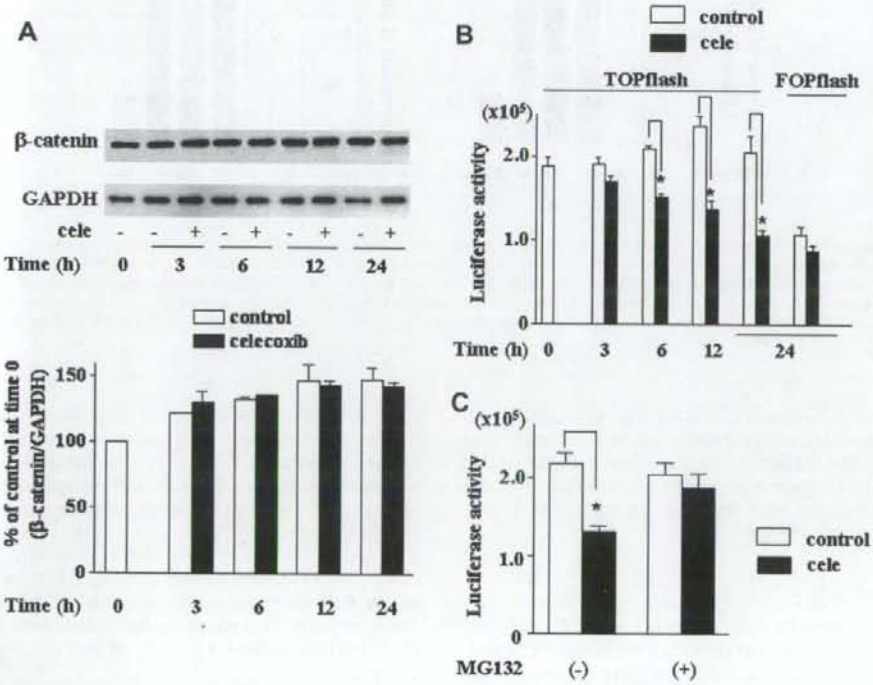

Fig. 3. The effect of celecoxib on β-catenin/TCF-dependent transcriptional activity. (A) Western blot analysis for β-catenin. HCT-116 cells were incubated with or without celecoxib (100 μM) for the period indicated. Protein samples were collected and separated by 12% SDS–PAGE and immunoblotted with the anti-β-catenin antibody. The membrane was reprobed with the anti-GAPDH antibody. The levels of protein bands were quantified and normalized to those of GAPDH. The results are shown as a percentage of the control level at time 0. Values are the means ± SE of three independent experiments. (B) Reporter gene assay with TOPFlash and FOPFlash. TOPflash or FOPflash was co-transfected with pRL-SV40 into HCT-116 cells. After 24-h incubation, cells were stimulated with or without celecoxib (100 μM) for the period indicated. Values are the means ± SE of three independent experiments performed in duplicate. $^{*}p < 0.01$ vs. control (Student's *t*-test). (C) MG132 inhibited the effect of celecoxib. TOPflash was co-transfected with pRL-SV40 into HCT-116 cells. After a 24-h incubation, cells were pretreated with or without 10 μM of MG132 for 1 h and then stimulated with or without 100 μM of celecoxib for 6 h. Values are the means ± SE of three independent experiments performed in duplicate. $^{*}p < 0.01$ vs. control (Student's *t*-test), cele: celecoxib.

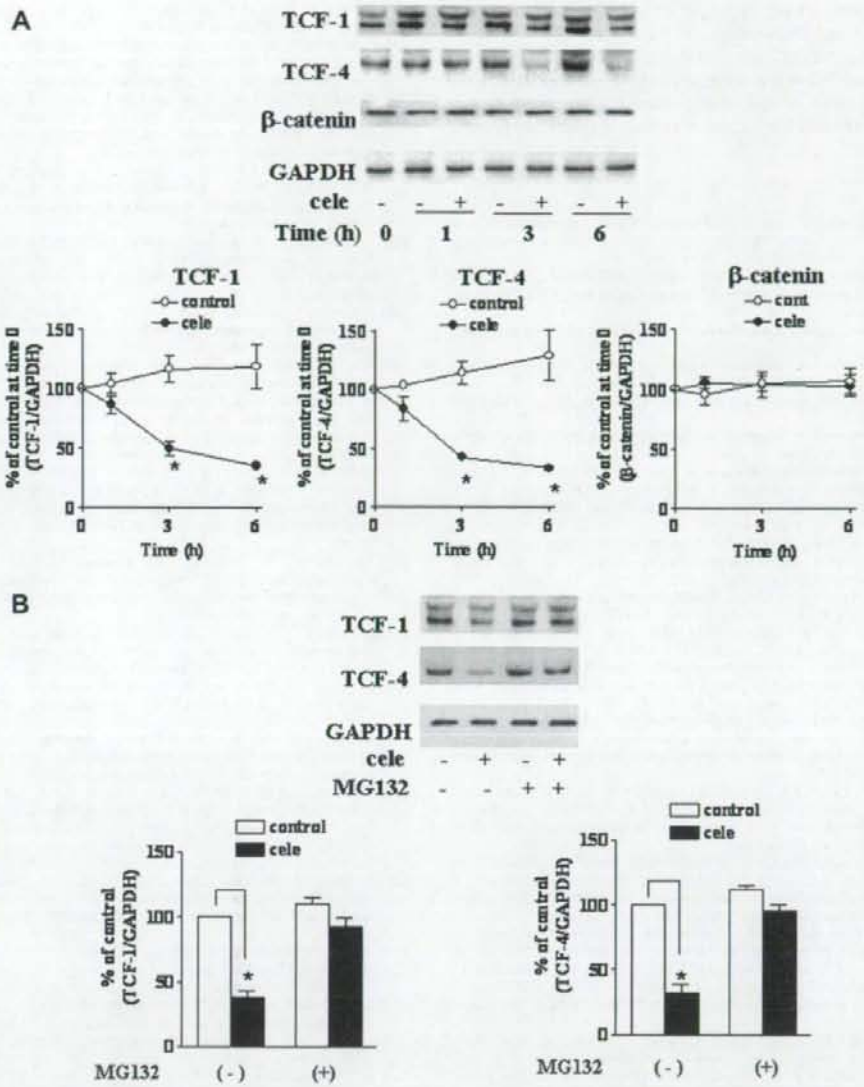

Fig. 4. The effect of celecoxib on the expression of TCF-1 and TCF-4 in DLD-1 cells. (A) Effect of celecoxib on TCFs expression in DLD-1 cells. DLD-1 cells were incubated with or without celecoxib (200 μM) for the indicated period. Protein samples were collected and separated by 12% SDS–PAGE and immunoblotted with anti-TCF-1, anti-TCF-4, anti-β-catenin and anti-GAPDH antibodies. The levels of protein bands were quantified and normalized to those of GAPDH. (B) MG132 inhibits TCFs degradation induced by celecoxib. HCT-116 cells were incubated with or without 10 μM MG132 for 1 h and stimulated with or without celecoxib (200 μM) for 6 h. Protein samples were collected and separated by 12% SDS–PAGE and immunoblotted with anti-TCF-1, anti-TCF-4, anti-β-catenin and anti-GAPDH antibodies. The levels of protein bands were quantified and normalized to those of GAPDH. The results are shown as a percentage of the control level. Values are the means ± SE of three independent experiments. $^{*}p < 0.01$ vs. control (Student's *t*-test), cele: celecoxib.

are known as COX-2-deficient cell lines [26,27], and not only COX-2 inhibitor but also COX-1 inhibitor (SC-560) induced degradation of TCF-1 and TCF-4. Thus celecoxib could induce degradation of TCF family members via COX-2-independent mechanisms.

There are at least 16 different variants of TCF-1, the molecular weights of which from 28 to 54 kDa, due to alternative splicing and promoter usage [31,32]. Half of them have a β-catenin binding domain (1–50 bp) (L-type, 1L–8L variants) which work as β-catenin/TCF-dependent transcriptional activators and the other half fail to bind β-catenin, because they lack the N-terminal region (1–114 bp) (S-type, 1S–8S variants), and act as a dominant-negative form of TCF-1 to inhibit β-catenin/TCF-dependent transcriptional activity [33,34]. Therefore, it might be important to clarify if celecoxib induces both L-type and S-type degradation. Although we could not clearly address which variant of the TCF-1 we detected at present, we might only be able to detect L-type variants of TCF-1 because of the anti-TCF-1 antibody we used is raised against the N-terminal region. In the case of TCF-4, there are 10 variants, molecular weights of which from 50 to 68 kDa, and all of which can bind to β-catenin to act as β-catenin/TCF-dependent transcriptional activators [35]. As 5 of 10 variants have almost same molecular weight (approx. 67 kDa) and the antibody we used could

recognize all variants, we are uncertain which TCF-4 variant we detected in HCT-116 and DLD-1 cells.

In summary, our results indicated that celecoxib induces degradation of TCF-1 and TCF-4 transcription factors and suppresses the transcriptional activity of the Wnt/β-catenin signaling pathway without affecting the level of β-catenin protein in colon cancer cells.

References

[1] P.J. Morin, A.B. Sparks, V. Korinek, N. Barker, H. Clevers, B. Vogelstein, K.W. Kinzler, Activation of β-catenin-Tcf signaling in colon cancer by mutations in β-catenin or APC, Science 275 (1997) 1787–1790.

[2] A.B. Sparks, P.J. Morin, B. Vogelstein, K.W. Kinzler, Mutational analysis of the APC/β-catenin/Tcf pathway in colorectal cancer, Cancer Res. 58 (1998) 1130–1134.

[3] M. Bienz, H. Clevers, Linking colorectal cancer to Wnt signaling, Cell 103 (2000) 311–320.

[4] S. Segditsas, I. Tomlinson, Colorectal cancer and genetic alterations in Wnt pathway, Oncogene 25 (2006) 7531–7537.

[5] T. Reya, H. Clevers, Wnt signalling in stem cells and cancer, Nature 434 (2005) 843–850.

[6] J. Taipale, P.A. Beachy, The hedgehog and Wnt signalling pathways in cancer, Nature 411 (2001) 349–354.

[7] M. Kitagawa, S. Hatakeyama, M. Shirane, M. Matsumoto, N. Ishida, K. Hattori, I. Nakamichi, A. Kikuchi, K. Nakayama, K. Nakayama, An F-box protein, FWD1, mediates ubiquitin-dependent proteolysis of β-catenin, EMBO J. 18 (1999) 2401–2410.

[8] C. Liu, Y. Li, M. Semenov, C. Han, G.H. Baeg, Y. Tan, Z. Zhang, X. Lin, X. He, Control of β-catenin phosphorylation/degradation by a dual-kinase mechanism, Cell 108 (2002) 837–847.

[9] M.J. Thun, M.M. Namboodiri, C.W. Jr. Heath, Aspirin use and reduced risk of fatal colon cancer, N. Engl. J. Med. 325 (1991) 1593–1596.

[10] T.A. Chan, Nonsteroidal anti-inflammatory drugs, apoptosis, and colon-cancer chemoprevention, Lancet Oncol. 3 (2002) 166–174.

[11] M.J. Thun, S.J. Henley, C. Patrono, Nonsteroidal anti-inflammatory drugs as anticancer agents: mechanistic, pharmacologic, and clinical issues, J. Natl. Cancer Inst. 94 (2002) 252–266.

[12] F.M. Giardiello, S.R. Hamilton, A.J. Krush, S. Piantadosi, L.M. Hylind, P. Celano, S.V. Booker, C.R. Robinson, G.J. Offerhaus, Treatment of colonic and rectal adenomas with sulindac in familial adenomatous polyposis, N. Engl. J. Med. 328 (1993) 1313–1316.

[13] G. Steinbach, P.M. Lynch, R.K. Phillips, M.H. Wallace, E. Hawk, G.B. Gordon, N. Wakabayashi, B. Saunders, Y. Shen, T. Fujimura, L.K. Su, B. Levin, The effect of celecoxib, a cyclooxygenase-2 inhibitor, in familial adenomatous polyposis, N. Engl. J. Med. 342 (2000) 1946–1952.

[14] R.S. Sandler, S. Halabi, J.A. Baron, S. Budinger, E. Paskett, R. Keresztes, N. Petrelli, J.M. Pipas, D.D. Karp, C.L. Loprinzi, G. Steinbach, R. Schilsky, A randomized trial of aspirin to prevent colorectal adenomas in patients with previous colorectal cancer, N. Engl. J. Med. 348 (2003) 883–890.

[15] J.A. Baron, B.F. Cole, R.S. Sandler, R.W. Haile, D. Ahnen, R. Bresalier, G. McKeown-Eyssen, R.W. Summers, R. Rothstein, C.A. Burke, D.C. Snover, T.R. Church, J.I. Allen, M. Beach, G.J. Beck, J.H. Bond, T. Byers, E.R. Greenberg, J.S. Mandel, N. Marcon, L.A. Mott, L. Pearson, F. Saibil, R.U. van Stolk, A randomized trial of aspirin to prevent colorectal adenomas, N. Engl. J. Med. 348 (2003) 891–899.

[16] S. Arico, S. Pattingre, C. Bauvy, P. Gane, A. Barbat, P. Codogno, E. Ogier-Denis, Celecoxib induces apoptosis by inhibiting 3-phosphoinositide-dependent protein kinase-1 activity in the human colon cancer HT-29 cell line, J. Biol. Chem. 277 (2002) 27613–27621.

[17] H.C. Lee, I.C. Park, M.J. Park, S. An, S.H. Woo, H.O. Jin, H.Y. Chung, S.J. Lee, H.S. Gwak, Y.J. Hong, D.H. Yoo, C.H. Rhee, S.I. Hong, Sulindac and its metabolites inhibit invasion of glioblastoma cells via down-regulation of Akt/PKB and MMP-2, J. Cell Biochem. 94 (2005) 597–610.

[18] E.M. Boon, J.J. Keller, T.A. Wormhoudt, F.M. Giardiello, G.J. Offerhaus, R. van der Neut, S.T. Pals, Sulindac targets nuclear β-catenin accumulation and Wnt signalling in adenomas of patients with familial adenomatous polyposis and in human colorectal cancer cell lines, Br. J. Cancer 90 (2004) 224–229.

[19] S. Dihlmann, A. Siermann, M. von Knebel Doeberitz, The nonsteroidal anti-inflammatory drugs aspirin and indomethacin attenuate β-catenin/TCF-4 signaling, Oncogene 20 (2001) 645–653.

[20] G. Hawcroft, M. D'Amico, C. Albanese, A.F. Markham, R.G. Pestell, M.A. Hull, Indomethacin induces differential expression of β-catenin, γ-catenin and T-cell factor target genes in human colorectal cancer cells, Carcinogenesis 23 (2002) 107–114.

[21] S. Dihlmann, S. Klein, M. von Knebel Doeberitz, Reduction of β-catenin/T-cell transcription factor signaling by aspirin and indomethacin is caused by an increased stabilization of phosphorylated β-catenin, Mol. Cancer Ther. 2 (2003) 509–516.

[22] S. Grösch, T.J. Maier, S. Schiffmann, G. Geisslinger, Cyclooxygenase-2 (COX-2)-independent anticarcinogenic effects of selective COX-2 inhibitors, J. Natl. Cancer Inst. 98 (2006) 736–747.

[23] A.H. Schönthal, Direct non-cyclooxygenase-2 targets of celecoxib and their potential relevance for cancer therapy, Br. J. Cancer 97 (2007) 1465–1468.

[24] N. Sakoguchi-Okada, F. Takahashi-Yanaga, K. Fukada, F. Shiraishi, Y. Taba, Y. Miwa, S. Morimoto, M. Iida, T. Sasaguri, Celecoxib inhibits the expression of survivin via the suppression of promoter activity in human colon cancer cells, Biochem. Pharmacol. 73 (2007) 1318–1329.

[25] M. Yamada, J. Ohnishi, B. Ohkawara, S. Iemura, K. Satoh, J. Hyodo-Miura, K. Kawachi, T. Natsume, H. Shibuya, NARF, an nemo-like kinase (NLK)-associated ring finger protein regulates the ubiquitylation and degradation of T cell factor/lymphoid enhancer factor (TCF/LEF), J. Biol. Chem. 281 (2006) 20749–20760.

[26] T.J. Maier, K. Schilling, R. Schmidt, G. Geisslinger, S. Grösch, Cyclooxygenase-2 (COX-2)-dependent and -independent anticarcinogenic effects of celecoxib in human colon carcinoma cells, Biochem. Pharmacol. 67 (2004) 1469–1478.

[27] S. Grösch, I. Tegeder, E. Niederberger, L. Bräutigam, G. Geisslinger, COX-2 independent induction of cell cycle arrest and apoptosis in colon cancer cells by the selective COX-2 inhibitor celecoxib, FASEB J. 15 (2001) 2742–2744.

[28] M. Ilyas, I.P. Tomlinson, A. Rowan, M. Pignatelli, W.F. Bodmer, B-catenin mutations in cell lines established from human colorectal cancers, Proc. Natl. Acad. Sci. USA 94 (1997) 10330–10334.

[29] I. Shureiqi, D. Chen, R. Lotan, P. Yang, R.A. Newman, S.M. Fischer, S.M. Lippman, 15-lipoxygenase-1 mediates nonsteroidal anti-inflammatory drug-induced apoptosis independently of cyclooxygenase-2 in colon cancer cells, Cancer Res. 60 (2000) 6846–6850.

[30] F. Takahashi-Yanaga, Y. Taba, Y. Miwa, Y. Kubohara, Y. Watanabe, M. Hirata, S. Morimoto, T. Sasaguri, Dictyostelium differentiation-inducing factor-3 activates glycogen synthase kinase-3β and degrades cyclin D1 in mammalian cells, J. Biol. Chem. 278 (2003) 9663–9670.

[31] K. Mayer, E. Wolff, H. Clevers, W.G. Ballhausen, The human high mobility group (HMG)-box transcription factor TCF-1:novel isoforms due to alternative splicing and usage of a new exon IXA, Biochim. Biophys. Acta 1263 (1995) 169–172.

[32] M. van de Wetering, J. Castrop, V. Korinek, H. Clevers, Extensive alternative splicing and dual promoter usage generate Tcf-1 protein isoforms with differential transcription control properties, Mol. Cell. Biol. 16 (1996) 745–752.

[33] M. van Noort, H. Clevers, TCF transcription factors, mediators of Wnt-signaling in development and cancer, Dev. Biol. 244 (2002) 1–8.

[34] L. Arce, N.N. Yokoyama, M.L. Waterman, Diversity of LEF/TCF action in development and disease, Oncogene 25 (2006) 7492–7504.

[35] A. Duval, S. Rolland, E. Tubacher, H. Bui, G. Thomas, R. Hamelin, The human T-cell transcriptional factor-4 gene: structure, extensive characterization of alternative splicings, and mutational analysis in colorectal cancer cell lines, Cancer Res. 60 (2000) 3872–3879.

Cardiovascular Research (2008) 77, 809–818
doi:10.1093/cvr/cvm095

Aryl hydrocarbon receptor mediates laminar fluid shear stress-induced CYP1A1 activation and cell cycle arrest in vascular endothelial cells

Zhiyi Han[1], Yoshikazu Miwa[1]*, Hiyo Obikane[2], Masako Mitsumata[2], Fumi Takahashi-Yanaga[1], Sachio Morimoto[1], and Toshiyuki Sasaguri[1]

[1]*Department of Clinical Pharmacology, Faculty of Medical Sciences, Kyushu University, 3-1-1 Maidashi, Higashi-ku, Fukuoka 812-8582, Japan; and* [2]*Department of Pathology, Nihon University School of Medicine, Tokyo, Japan*

Received 10 April 2007; revised 19 November 2007; accepted 30 November 2007; online publish-ahead-of-print 7 December 2007

Time for primary review: 29 days

KEYWORDS
Aryl hydrocarbon receptor;
CYP1A1;
Shear stress;
Cell cycle;
Endothelial cell

Aims We investigated the mechanisms of shear stress (SS)-induced activation of cytochrome P450 (CYP) 1A1 and cell cycle arrest with regard to the role of the aryl hydrocarbon receptor (AhR), since AhR mediates the expression of CYP1A1 induced by polycyclic aromatic hydrocarbons (PAHs) and is thought to be involved in the regulation of cell growth and differentiation.

Methods and results Human umbilical vein endothelial cells (ECs) were exposed to laminar SS and thereafter collected to evaluate the expression, activity, and transcription of CYP1A1 and the expression of AhR and cell cycle-related proteins. A physiological level of laminar SS (15 dynes/cm^2) markedly increased the expression level and enzymatic activity of CYP1A1. SS stimulated CYP1A1 promoter activity without influencing mRNA stability. Loss of two functional xenobiotic response elements (XREs) in the 5′-flanking region of the CYP1A1 gene suppressed the SS-induced transcription of CYP1A1. Laminar SS stimulated the expression and nuclear translocation of AhR. α-Naphthoflavone, an AhR antagonist, and a small interfering RNA (siRNA) for AhR significantly suppressed SS-induced CYP1A1 expression. The siRNA also abolished SS-induced cell cycle arrest, the expression of the cyclin-dependent kinase inhibitor $p21^{Cip1}$, and dephosphorylation of retinoblastoma protein.

Conclusion Laminar SS stimulated the transcription of CYP1A1 through the activation of AhR in a way that is similar to the effects of PAHs. AhR was also involved in cell cycle arrest induced by SS. Our results suggest that sustained activation of AhR exposed to blood flow plays an important role in the regulation of EC functions.

1. Introduction

Aryl hydrocarbon receptor (AhR), a ligand-activated transcription factor, plays a central role in the induction of cytochrome P450 (CYP), especially CYP1A1, an enzyme produced on exposure to polycyclic aromatic hydrocarbons (PAHs) such as benzo(a)pyrene and 2,3,7,8-tetrachlorodibenzo-*p*-dioxin (TCDD).[1,2] On binding to AhR, PAHs translocate the receptor from the cytoplasm into the nucleus, where it forms a heterodimer with AhR nuclear translocator protein (ARNT). The dimer binds to the xenobiotic response elements (XREs) in the promoter region of the CYP1A1 gene to activate CYP1A1 transcription.[3] CYP1A1 generates harmful bioactive substances by metabolizing PAHs, and therefore, it is believed that AhR activation and subsequent CYP1A1 induction are aetiological factors for diseases such as cancers and atherosclerosis.[4]

In contrast, AhR is reported to contribute to normal physiological processes during cell growth and differentiation.[5] AhR-knockout mice exhibit a number of phenotypic abnormalities such as peripheral immune system deficiency, liver defects, and hypertrophic and fibrotic changes of the cardiovascular system, although the mice are resistant to TCDD toxicity.[6] In cultured cells, several studies suggest that the activation of AhR is involved in cell cycle arrest in the absence or presence of exogenous agonists.[7–9] These observations suggest that AhR may have important roles in physiological functions.

CYP1A1 is constitutively expressed in vascular endothelium *in vivo*[10]; however, the involvement of AhR has not been fully investigated. Vascular endothelial cells (ECs) are constantly exposed to haemodynamic forces, such as fluid shear stress (SS). Laminar SS plays an essential

* Corresponding author. Tel: +81 92 642 6082; fax: +81 92 642 6084.
E-mail address: ymiwa@clipharm.med.kyushu-u.ac.jp

role in the maintenance of the structure and function of blood vessels by regulating the expression of numerous genes and proteins.[11] Recent studies show that laminar SS strongly induces the expression of CYP1A1 in vascular ECs.[12,13] However, in spite of this, evidence suggests that laminar blood flow is atheroprotective.[14,15] Atherosclerosis tends to occur in areas exposed to disturbed flow or low SS, and a lack of SS induces apoptosis in ECs.[16] Therefore, we believe that the SS-induced sustained expression of CYP1A1 may have an important physiological role, in contrast to the transient induction by PAHs. In fact, loss of CYP1A1 is reported to correlate with dedifferentiation of cultured rat aortic ECs.[17]

Thus, in the present study, we examined the mechanism of expression of CYP1A1 induced by laminar SS in relation to the involvement of AhR in vascular ECs. Since we have reported that SS inhibits EC proliferation by inducing the expression of the cyclin-dependent kinase inhibitor $p21^{Cip1}$,[18] we also investigated the relationship between AhR and SS-induced cell cycle inhibition.

2. Methods

2.1 Chemicals

Actinomycin D (Act D), alpha-naphthoflavone (α-NF), and SB203580 were purchased from Sigma. U0126 was purchased from Cell Signaling Technology. SP600125 was purchased from LC Laboratories.

2.2 Cell culture

Human umbilical vein ECs (HUVECs) were isolated by collagenase digestion and cultured as described previously.[19] Human umbilical cords were obtained from healthy women who underwent uncomplicated term pregnancies. This investigation conforms to the principles outlined in the Declaration of Helsinki. Informed consent was obtained from each donor. Bovine arterial ECs (BAECs) were grown in Dulbecco's modified Eagle's medium containing 10% (v/v) foetal bovine serum (Hyclone), 100 U/mL penicillin, 100 mg/mL streptomycin, and 1 mg/mL amphoteracin B. Cells were used for experiments between passages 2 and 10.

2.3 Shear stress experiments

The laminar flow experiments were performed using a parallel plate chamber as described previously.[18] Briefly, cells were grown on gelatin-coated polyester sheets (Plastic Suppliers) until confluent. Control cells (static cells) were grown on the same polyester sheets in the same medium as sheared cells until confluent, and were transferred into fresh medium before being maintained in an incubator. A confluent monolayer of ECs on a polyester sheet was placed in a parallel-plate flow chamber and subjected to steady laminar shear stress. The flow loop with reservoirs and the flow chamber were filled with DMEM containing 10% foetal bovine serum.

To compare the effects of laminar and turbulent SS on the expression of CYP1A1 and AhR, a cone-plate type apparatus was used as previously described.[20] Cells were grown on a 10 cm dish until confluent and then exposed to laminar or turbulent SS using 0.5° or 5° cones, respectively, with a rotational velocity of 120 r.p.m. From the calculated modified Reynolds number (R'), turbulent flow was established at radii ≥2.4 cm, which corresponded to an $R' > 5$ and represented an average SS strength of 1.5 dyne/cm^2. Laminar SS strength was 6 dyne/cm^2. Cells were harvested from only the outer portion of the glass plate (≥2.4 cm).

2.4 Western blot analysis

Western blotting was performed as described previously,[21] using a polyclonal anti-CYP1A1 antibody (Santa Cruz Biotechnology), polyclonal anti-AhR antibody (Santa Cruz Biotechnology), polyclonal anti-ERK/phospho-ERK antibody (Cell Signaling Technology), monoclonal anti-JNK antibody and polyclonal anti-phospho-JNK antibody (Cell Signaling Technology), polyclonal anti-p38 mitogen-activated protein kinase (MAPK)/phospho-p38 MAPK antibody (Santa Cruz Biotechnology), polyclonal anti-$p21^{Cip1}$ antibody (Santa Cruz), and monoclonal anti-pRb antibody (Pharmingen). Nucleic and cytoplasmic proteins were purified using a Nuclear and Cytoplasmic Extraction Reagents kit (PIERCE), following the manufacturer's instructions. Membranes were re-probed with anti-β-actin monoclonal antibody to normalize the amounts of proteins applied to the SDS–PAGE gel, (Calbiochem).

2.5 Reverse transcription–polymerase chain reaction

Total cellular RNA was extracted with TRIzol Reagent (Invitrogen). The expression of mRNA was analysed by reverse transcription–polymerase chain reaction (RT–PCR) using Ready-To-Go RT–PCR Beads (Amersham Biosciences). The primers for human CYP1A1 and GAPDH were synthesized based on information obtained from the GenBank database: CYP1A1, 5′-GGATCTTTCTCTGTACCCTGG-3′ and 5′-AGCATGTCCTTCAGCCCAGA-3′; GAPDH, 5′-TCCACCACCCTGTTG CTGTA-3′ and 5′-ACCACAGTCCATGCCATCAC-3′; bovine CYP1A1, 5′-TCGGGCACATGCTGATGTTG-3′ and 5′-GCACAGATGACATTGGCC ACTG-3′; and bovine GAPDH 5′-AAGGCAGAGAACGGGAAGCT-3′ and 5′-TCCCTCCACGATGCCAAAGT-3′.

2.6 Measurement of CYP1A1 activity

CYP1A1 activity was evaluated with the ethoxyresorufin-*O*-dealkylase (EROD) assay, which measures the ability to convert ethoxyresorufin to resorufin, as described previously.[22]

2.7 Construction of plasmids and mutagenesis

The 5′-flanking region of rat CYP1A1 gene (−1166/+18) was amplified by PCR with 5′-GGTGAGATCTGCGCCCTTGCAAAGCTTAAGACTA-3′ as a sense primer and 5′-GGAGGAGCTTGGCACCACCACCTTTATATG-3′ as an antisense primer, and subcloned into the SacI/XhoI sites of a PGL3-basic luciferase-expressing reporter vector (Promega), a firefly luciferase reporter vector. For the two deletion constructs (DM-1 and DM-2), two restriction enzyme-digested fragments (DM-1, SacI/Bst1107I −859/+18; DM-2, SacI/BstEII −206/+18) were blunted and ligated using a DNA Blunting Kit (Takara). Site-directed mutagenesis was performed using QuickChange Site-directed Mutagenesis Kit (Stratagene), as instructed by the manufacturer. The luciferase reporter construct containing the −1166/+18 region of the CYP1A1 promoter was used as a DNA template. The mutations introduced into the putative binding sites for XRE were as follows: Mut-1 (−1069/−1052) CCCCCAGCTAGCGTGA CA→CCCCCAGCTAGTTAGACA; Mut-2 (−987/−970), TCTCACG CAACTCCGGGG→TCTCTAACAACTCCGGGG. Mut-3 has both mutations. The structure of every DNA construct was verified by sequencing.

siRNA duplexes were prepared by SAMCHULLY and targeted the coding regions of bovine AhR mRNA (770–778). The siRNA duplexes used in this study were as follows: siRNA for AhR (si-AhR), 5′-UACUUCCACCUCAGUUGGCTT-3′ and 5′-GCCAACUGAGGUGGAA GUATT-3′; Scramble (si-Scr), 5′-GCGCGCUUUGUAGGAUUCGTT-3′ and 5′-CGAAUCCUACAAAGCGCGCTT-3′, respectively.

2.8 Transfection and luciferase reporter assay

Transfection and luciferase reporter assays were performed as described.[23] Since we failed to amplify the fragment of human

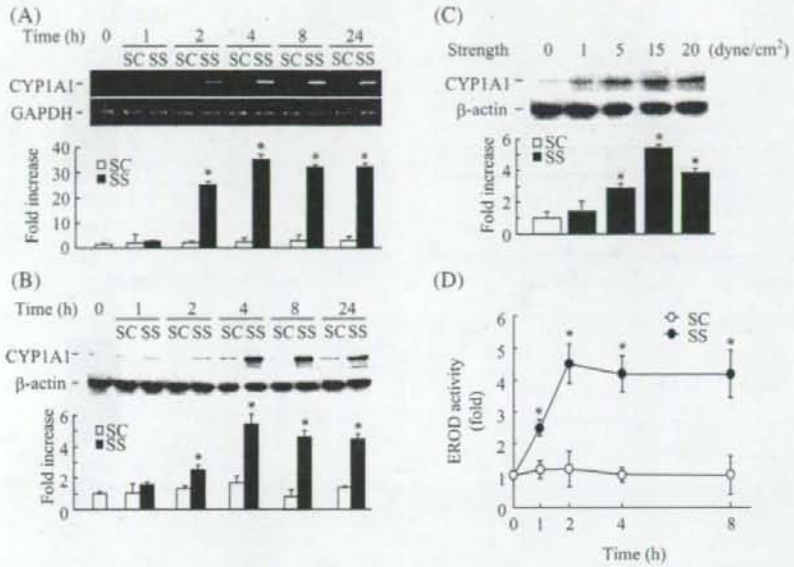

Figure 1 Effects of shear stress (SS) on the expression and activity of CYP1A1 in endothelial cells. Human umbilical vein endothelial cells (HUVECs) were maintained in static conditions (SC) or exposed to laminar SS (SS, 15 dyne/cm^2) for the periods indicated (*A and B*). (*A*) CYP1A1 mRNA expression was analysed by reverse transcription-polymerase chain reaction (RT-PCR). (*B*) The time-course of CYP1A1 protein expressions induced by SS. (*C*) Strength dependency of CYP1A1 induction by laminar SS. HUVECs were exposed to laminar SS for 4 h at the indicated strengths. (*D*) CYP1A1 enzymatic activity in HUVECs was analysed by EROD assay as described in 'Methods' and plotted as a percentage of the value obtained in cells cultured under SC at time 0. Error bars represent the SD values obtained from four independent experiments. *$P < 0.01$ vs. SC. (*E*) HUVECs were exposed to SS for 4 h and thereafter treated with actinomycin D (Act D, 3 μmol/L), and incubated in static conditions (SC + Act D), or exposed to SS (SS + Act D). Expression levels of CYP1A1 mRNA normalized to those of GAPDH mRNA were standardized to the values obtained at the start time (−4 h), and the time-course after the administration of Act D is plotted in the lower panel. Error bars represent the SD values obtained from four independent experiments. (*F*) HUVECs (upper panel) or bovine arterial endothelial cells (BAECs) (lower panel) transfected with the plasmid containing the −1116/+18 region of the rat CYP1A1 promoter together with pRL-SV40 were incubated in SC, or exposed to laminar SS for 8 h. Mean raw values of firefly (CYP1A1) or renilla (control) luciferase activity are indicated below the panel. Relative luciferase activity is presented as the fold increase against the value obtained under SC. Data represent means ± SD of four independent experiments. *$P < 0.01$. (*G*) BAECs were maintained in SC or exposed to laminar SS (SS, 15 dyne/cm^2) for the periods indicated. *Upper panel*: CYP1A1 mRNA expression was analysed by RT-PCR. *Lower panel*: CYP1A1 protein expression was analysed by western blotting. Error bars represent the SD values obtained from four independent experiments. *$P < 0.01$ vs. SC. (*H*) CYP1A1 enzymatic activity in BAECs maintained in SC or exposed to laminar SS (SS, 15 dyne/cm^2) was analysed and plotted as described in *D*. *$P < 0.01$ vs. SC.

CYP1A1 promoter, we used rat CYP1A1 promoter in these assays because it has a high homology with the human CYP1A1 promoter. This is especially true of the four XRE motifs which show 93.3% (the first XRE), 92.9% (the second XRE), 93.1% (the third XRE), and 93.9% (the fourth XRE) homology. Excepting *Figure 1F*, promoter constructs were transfected into BAECs, because the efficiency of the transfection was much higher in BAECs (~70%) than in HUVECs (~20%). Cells were transiently transfected with plasmid DNA using LipofectAMINE regent (Life Technologies) as per the manufacturer's instructions. Simultaneously, pRL-simian virus 40 (pRL-SV40), which contained a Renilla luciferase gene with an SV40 promoter, was co-transfected as a control for transfection efficacy. Luciferase activity was measured using a double luciferase assay system (Toyo Ink Manufacturing Co.) and a Lumat LB9507 luminometer (Berthold Technologies). Firefly luciferase activity was normalized to Renilla luciferase activity to determine relative luciferase activity.

2.9 Fluorescence microscopy

After stimulation, the cells were fixed in ice-cold methanol/acetone (1:1) for 15 min at −20°C and then washed twice with phosphate-buffered saline. After blocking with 2% bovine serum albumin in phosphate-buffered saline for 30 min, cells were incubated overnight with polyclonal anti-AhR antibody (Santa Cruz Biotechnology, 1:200) at 4°C. Thereafter, cells were washed twice with phosphate-buffered saline and incubated with anti-rabbit IgG + IgA + IgM-biotin (Nichirei) for 1 h at room temperature, followed by streptavidin-fluorescein isothiocyanate conjugate (1:50 dilution; Invitrogen) for 1 h at room temperature. The cells were examined under a fluorescence microscope (Olympus).

2.10 Cell proliferation assay

To assess EC proliferation, we used the BrdU Cell Proliferation Assay (Exalpha Biologicals, Inc., MA, USA) according to the manufacturer's protocol. After stimulation, ECs were incubated overnight in culture medium containing BrdU (2 μl/ml). The uptake of BrdU was determined with a spectrophotometer (Bio-Tek Instruments, Highland Park, VT, USA) and normalized to the amount of cellular protein, which was measured in parallel samples according to the method of Lowry.

2.11 Statistics

Results are expressed as the mean ± SD of a number of the observations. Statistical significance was assessed by Student's *t*-test for paired or unpaired values.

3. Results

3.1 The induction and activation of CYP1A1 in response to shear stress

We first confirmed the effect of SS on the expression of CYP1A1 using HUVECs. Although the level of CYP1A1 mRNA

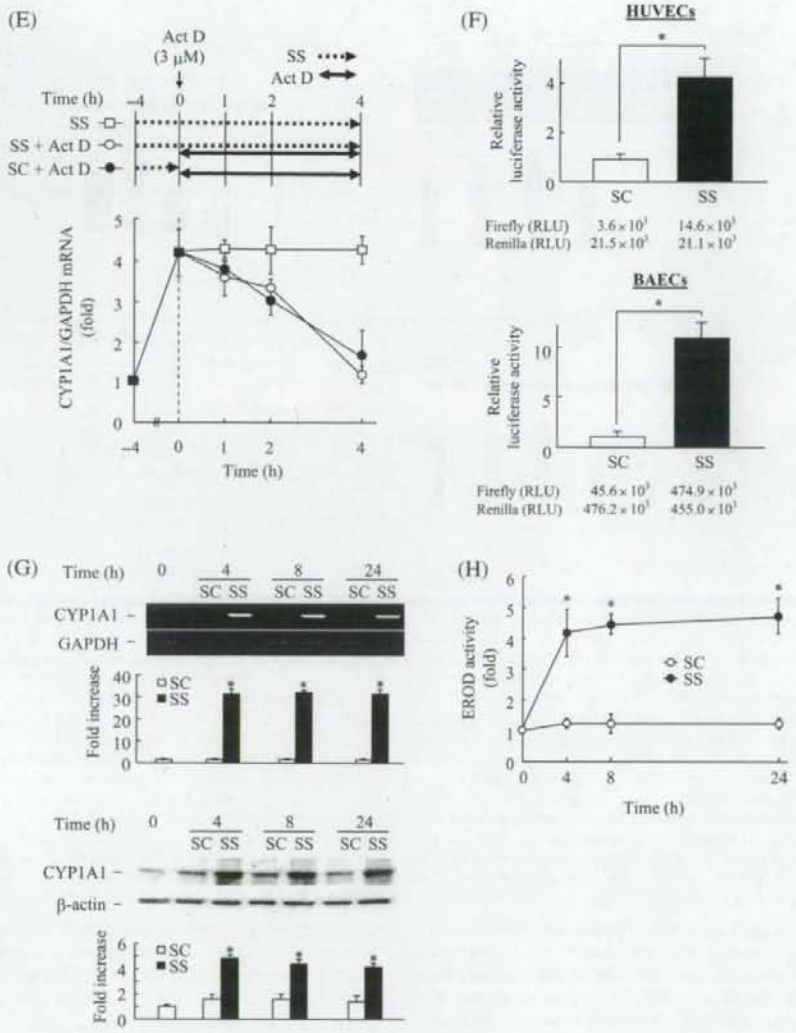

Figure 1 Continued.

was very low in static control cells, it rose markedly on exposure to a physiological level of laminar SS (15 dyne/cm^2) (*Figure 1A*), consistent with previous reports.[12,13] The expression of CYP1A1 protein was also increased by SS and sustained over 24 h (*Figure 1B*). This CYP1A1 induction was SS strength-dependent (*Figure 1C*) and the expression level reached a maximal at 15 dyne/cm^2. As shown in *Figure 1D*, CYP1A1 activity determined by EROD assay was also increased by SS and reached a plateau after 2 h.

To investigate the mechanism of SS-induced CYP1A1 expression, we measured the rate of decay of the CYP1A1 mRNA after the addition of actinomycin D (Act D, 3 μmol/L), a transcription inhibitor. The degradation rates did not differ between the cells exposed to SS and those cultured in static conditions (*Figure 1E*). We also examined the effect of SS on CYP1A1 gene transcription in HUVECs transfected with a luciferase reporter construct driven by the 5′-flanking region of the rat CYP1A1 gene (−1116/+18 bp). Although the obtained raw values of luciferase activity were relatively low, it was significantly enhanced in HUVECs after exposure to SS for 8 h (*Figure 1F*, upper panel). When we did the same experiment using BAECs, the values of luciferase activity were much higher than those in HUVECs and furthermore, relative luciferase activity was strongly enhanced by SS (10.9-fold) (*Figure 1F*, lower panel). In BAECs, laminar SS induced mRNA and protein expressions (*Figure 1G*) and increased enzymatic activity of CYP1A1 (*Figure 1H*) as well as in HUVECs. These results suggest that SS induces CYP1A1 expression by activating gene transcription. The following transfection experiments were done using BAECs because of their higher transfection efficiency.

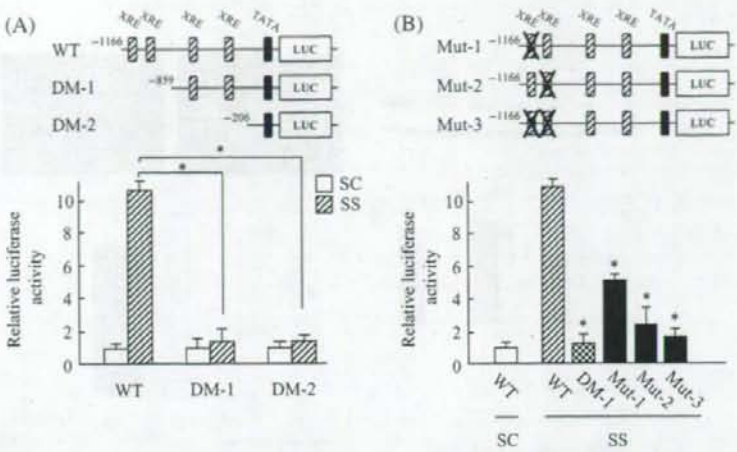

Figure 2 Analysis of the CYP1A1 gene promoter in response to shear stress (SS). (*A*) The wild-type (WT) construct contains −1116/+18 bp of the CYP1A1 promoter, deletion mutant-1 (DM-1) contains −859/+18 bp of the promoter without the distal two xenobiotic response elements (XREs), deletion mutant-2 (DM-2) contains −206/+18 bp of the promoter without all four XREs. TATA, TATA box; Luc, firefly luciferase reporter gene. Bovine arterial endothelial cells transfected with WT, DM-1, or DM-2 together with pRL-SV40 were incubated in static conditions (SC) or exposed to laminar SS (SS) for 8 h. Relative luciferase activity is presented as the fold increase over the value obtained in the control for WT. Data represent means ± SD of four independent experiments. *$P < 0.01$. (*B*) Site-mutated constructs (Mut-1, Mut-2, and Mut-3) were produced as described in 'Methods'. Bovine arterial endothelial cells transfected with Mut-1, Mut-2, or Mut-3, together with pRL-SV40, were exposed to SS for 8 h. Relative luciferase activity is presented as the fold increase over the value obtained in the SC for WT. Data represent means ± SD of four independent experiments. *$P < 0.01$ vs. SS for WT.

3.2 Xenobiotic response element mediates shear stress-induced CYP1A1 transcription

A number of studies have shown that PAHs stimulate CYP1A1 gene transcription through the XREs in the gene's promoter. SS activates the transcription of a variety of genes through several specific sequences; however, the SS-response element in the CYP1A1 promoter has not been identified. Therefore, we attempted to uncover the precise mechanism of SS-induced CYP1A1 expression by analysing the CYP1A1 gene promoter. Since there were four XREs in the rat CYP1A1 gene (−1116/+18 bp), we generated two deletion mutant constructs: DM-1 (−859/+18 bp) and DM-2 (−206/+18 bp). In BAECs transfected with these deletion mutants, the increase in luciferase activity was almost completely suppressed in comparison with the marked elevation in wild type (WT) (*Figure 2A*). This suggests that the main elements responsive to SS were located between bp −1116 and −859 in the 5′-flanking region, where two XREs exist.

Subsequently, we introduced mutations (Mut-1, Mut-2, and Mut-3) into these two upstream XREs to determine whether these sequences are responsible for SS-induced CYP1A1 expression. Mut1 and Mut2 significantly suppressed SS-induced CYP1A1 promoter activity, and Mut3, where both of the XREs were mutated, almost eliminated the response to SS (*Figure 2B*). These results suggest that both of these XREs are essential for CYP1A1 induction by SS.

3.3 Laminar shear stress induced the expression and nuclear translocation of aryl hydrocarbon receptor

The results suggested that SS activates CYP1A1 gene transcription through XREs in a similar way to PAHs. AhR is known to mediate PAH-induced transcriptional activation of the CYP1A1 gene. Therefore, we subsequently examined the effect of SS on AhR expression. As shown in *Figure 3A*, SS significantly increased the expression of AhR protein, as well as CYP1A1, and this induction was sustained over 24 h. Immunoblotting of the subcellular fractions revealed that AhR was predominantly in the cytoplasm with only a small amount present in the nucleus in static ECs; however, it was translocated from the cytoplasm into the nucleus after stimulation with SS (*Figure 3B*). The nuclear translocation of AhR by SS was confirmed by immunofluorescence staining (*Figure 3C*).

We also compared the effects of the physiological level of laminar and turbulent SS on the expression of AhR and CYP1A1, because atherosclerotic lesions tend to develop at arterial bifurcations and curvatures where laminar blood flow is often turbulent. As shown in *Figure 3D*, the physiological level of turbulent SS (average strength: 1.5 dyne/cm^2) induced AhR and CYP1A1, however; the induction was weaker than that by laminar SS (6 dyne/cm^2).

3.4 The aryl hydrocarbon receptor inhibitor alpha-naphthoflavone and aryl hydrocarbon receptor small interfering RNA suppressed laminar shear stress-induced CYP1A1 expression

We examined the effect of AhR inhibition to determine whether AhR is essential for the SS-induced expression of CYP1A1. Alpha-NF (10 μmol/L), an AhR inhibitor, strongly suppressed SS-induced CYP1A1 expression (*Figure 4A*). We also examined the effect of siRNA for AhR (si-AhR) and found that si-AhR significantly suppressed SS-induced expression of AhR, whereas scramble siRNA (si-Scr) did not (*Figure 4B*). When the AhR si-RNA was transfected into BAECs, SS-induced expression of CYP1A1 was strongly suppressed (*Figure 4C*).

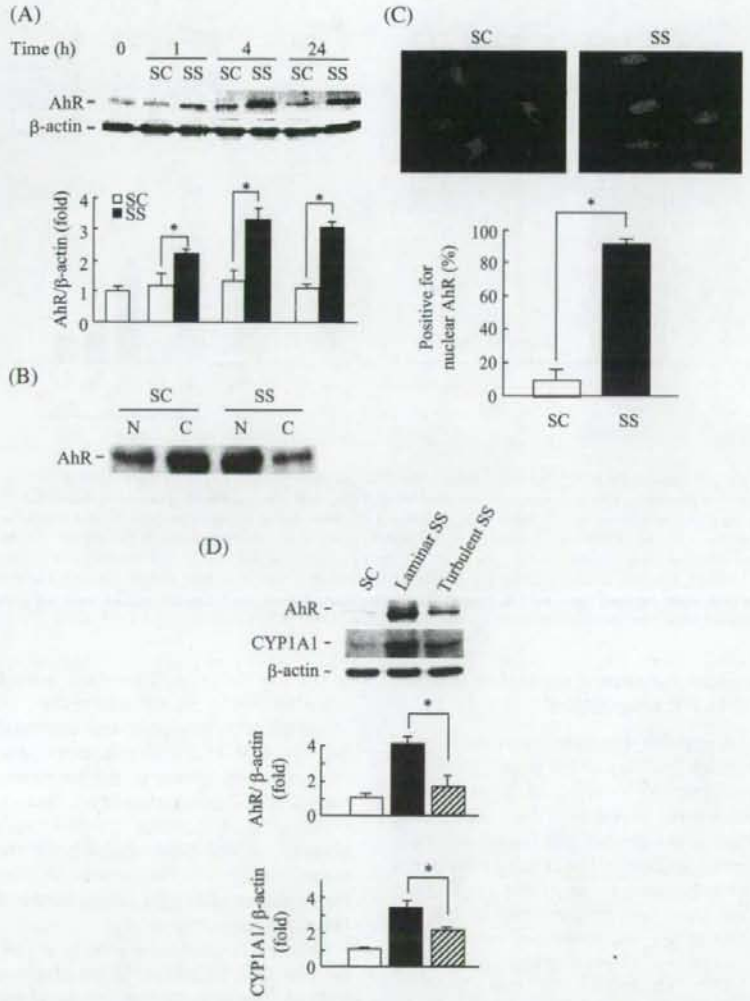

Figure 3 Effects of laminar shear stress (SS) on aryl hydrocarbon receptor (AhR) expression and nuclear translocation of AhR. (*A*) Human umbilical vein endothelial cells (HUVECs) were maintained in static conditions (SC) or exposed to laminar SS (15 dyne/cm^2) (SS) for the periods indicated. Expression levels of AhR protein normalized to those of β-actin protein were standardized to the values obtained at 0 h and shown as means ± SD of four independent experiments in the bar graph. *$P < 0.01$. (*B*) HUVECs were maintained in SC or exposed to laminar SS (15 dyne/cm^2) (SS) for 8 h. Nuclear (N) and cytoplasmic (C) proteins were purified as described under 'Methods'. (*C*) HUVECs were maintained in SC or exposed to laminar SS (15 dyne/cm^2) (SS) for 8 h. After stimulation, immunofluorescent staining with an anti-AhR antibody was performed as described under 'Methods'. Bar graph represents the percentages of cells positive for nuclear AhR staining. *$P < 0.01$. (*D*) HUVECs were exposed to laminar and turbulent SS for 4 h using a cone-plate type apparatus as described in 'Methods'. Expression levels of AhR protein or CYP1A1 protein normalized to those of β-actin protein were standardized to the values obtained from cells maintained in SC, and shown as means ± SD of three independent experiments in the bar graph. *$P < 0.01$.

3.5 Involvement of the mitogen-activated protein kinase pathways in shear stress-induced aryl hydrocarbon receptor expression

Several reports have suggested that MAPKs modulate AhR expression.[24–26] It has also been reported that SS activates MAPKs.[27–29] To elucidate the mechanism by which SS induces the expression of AhR, we examined the effect of SS on the phosphorylation of MAPKs, i.e. ERK, JNK, and p38. As shown in *Figure 5A*, the expression levels of these MAPKs were not altered by SS. However, the levels of phosphorylated JNK and p38 but not ERK were markedly elevated by SS. Importantly, these time-courses were similar to those of AhR and CYP1A1 expression induced by SS. We subsequently examined the effects of the MAPK inhibitors U0126 (ERK inhibitor), SP600125 (JNK inhibitor), and SB203580 (p38 inhibitor) on SS-induced expression of AhR and CYP1A1. Both SP600125 (*Figure 5B*) and SB203580 (*Figure 5C*) markedly reduced SS-induced expression of AhR and CYP1A1, whereas U0126 did not (*Figure 5D*). This suggests that SS induces expression of AhR through phosphorylation of JNK and p38, resulting in an increase in CYP1A1 expression.

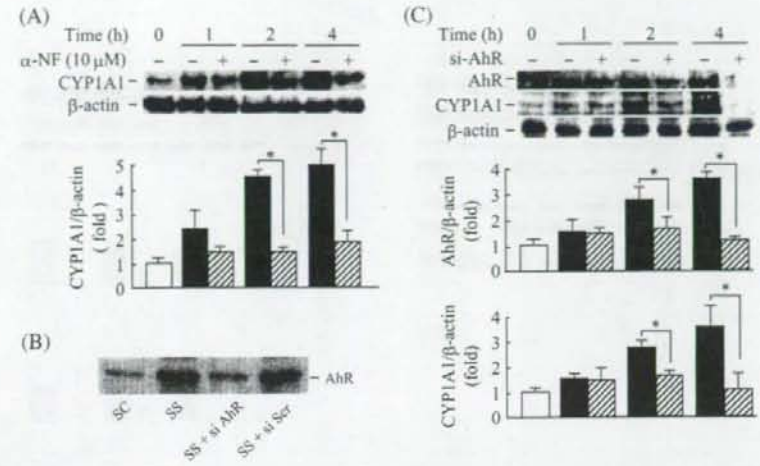

Figure 4 Effects of aryl hydrocarbon receptor (AhR) inhibition on the expressions of CYP1A1 induced by shear stress (SS). (*A*) Human umbilical vein endothelial cells were exposed to laminar SS (15 dyne/cm^2) in the absence or presence of alpha-naphthoflavone (10 μmol/L) for the periods indicated. Expression levels of CYP1A1 protein normalized to those of β-actin protein were standardized to the values obtained at 0 h, and shown as means ± SD of four independent experiments in the bar graph. *$P < 0.01$. (*B*) Bovine arterial endothelial cells (BAECs) transfected with small interfering RNA (siRNA) for AhR (si-AhR) or scramble RNA (si-Scr) were exposed to SS for 8 h. (*C*) BAECs transfected with si-AhR or si-Scr were exposed to laminar SS (15 dyne/cm^2) (SS) for the periods indicated. Expression levels of AhR protein or CYP1A1 protein normalized to those of β-actin protein were standardized to the values obtained at 0 h shown as means ± SD of four independent experiments in the bar graph. *$P < 0.01$.

3.6 Aryl hydrocarbon receptor mediates shear stress-induced cell cycle arrest

Previous studies suggest that there is a relationship between AhR and cell growth inhibition.[22,30] We reported that SS inhibits EC proliferation by inducing expression of the cyclin-dependent kinase inhibitor p21^{Cip1}.[18] To investigate whether AhR is involved in SS-induced cell cycle arrest in ECs, we examined the effects of si-AhR on the arrest. As shown in *Figure 6A*, si-AhR restored the ability to proliferate. SS induced p21^{Cip1} expression and suppressed phosphorylation of the retinoblastoma tumour suppressor protein (pRb) required for G_1/S transition consistent with our previous report.[18] However, both of these changes were reversed by treatment with si-AhR (*Figure 6B*).

4. Discussion

In this study, we showed for the first time that the expression of AhR is induced by laminar fluid SS, probably through activation of the JNK/p38 pathways, and leads to expression of the CYP1A1 gene through XRE-dependent transcription. Furthermore, we found that AhR is also involved in SS-induced cell cycle arrest. The induction of AhR and CYP1A1 by turbulent SS was weaker than that by laminar SS, suggesting that the expression of these proteins is involved in the maintenance of vascular homeostasis.

A physiological level of laminar SS strongly induced CYP1A1 expression in vascular ECs, consistent with previous reports,[12,13] and enhanced CYP1A1 activity. SS increased the activity of the CYP1A1 gene promoter; furthermore, deletion of parts of the 5′-flanking region of the CYP1A1 gene showed that the response to SS depended on the region between bp −1116 and −859, which contains two XREs. Mutations introduced into these two XREs almost completely abolished the SS-mediated response, suggesting that these XREs are essential for SS-induced transcription of the CYP1A1 gene.

Laminar SS induced the expression of AhR and facilitated its nuclear translocation required for binding to XREs (*Figure 3B* and *C*). The inhibition of AhR by α-NF or siRNA suppressed CYP1A1 induction by SS, suggesting that AhR mediates CYP1A1 induction by SS. Importantly, the induction patterns of AhR and CYP1A1 by SS were different from those by PAHs. Previous reports indicated that the expressions of AhR and CYP1A1 are transiently induced by PAHs within 1 h after stimulation, and thereafter expression rapidly declines.[31,32] However, laminar SS showed sustained induction of AhR and CYP1A1 until at least after 24 h in the present study. SS may continuously induce an unknown endogenous ligand that can bind and activate AhR. Considering the very low expression of AhR in ECs in static condition, AhR seems to be mainly regulated by SS in the vascular wall. Furthermore, the sustained induction of AhR and subsequent activation of CYP1A1 by SS may essentially indicate a physiological role, which is distinct from the effects of the vast majority of PAHs.

In addition, SS-induced AhR expression was probably mediated through the activation of the JNK/p38 pathways, since SS induced sustained activation of JNK and p38 (*Figure 5A*) and the inhibition of JNK or p38 suppressed the SS-induced expression of AhR and CYP1A1 (*Figure 5B* and *C*). However, SS did not activate ERK and U0126 failed to inhibit SS-induced expression of AhR and CYP1A1, suggesting that the ERK pathway is not required for this process, although several papers have reported an association between ERK and AhR activation.[33,34]

We previously reported that laminar SS induces cell cycle arrest in vascular ECs by inhibiting the transition from G_1 to S phase.[18] Since frequent cell division seems to increase the vascular wall permeability,[35] restricting the proliferation of EC would achieve the stabilization of ECs. In fact, early

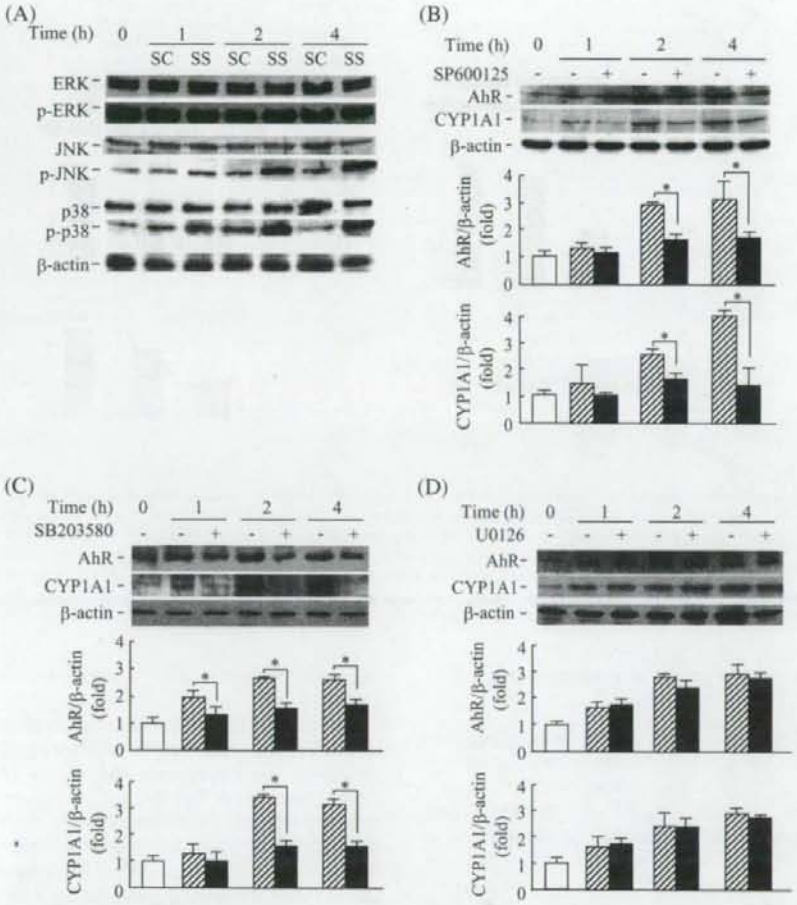

Figure 5 Effect of shear stress (SS) on the phosphorylation of mitogen-activated protein kinase (MAPKs). (*A*) Human umbilical vein endothelial cells (HUVECs) were maintained in static conditions (SC) or exposed to laminar SS (15 dyne/cm^2) (SS) for the periods indicated. Levels of MAPKs and phosphorylated (p-) MAPKs were analysed by western blotting. (*B*) HUVECs were exposed to laminar SS (15 dyne/cm^2) in the absence or presence of SP600125 for the periods indicated. Expression levels of aryl hydrocarbon receptor (AhR) protein or CYP1A1 protein normalized to those of β-actin protein were standardized to the values obtained at 0 h and shown as means ± SD of four independent experiments in the bar graph. *$P < 0.01$. (*C*) HUVECs were exposed to laminar SS (15 dyne/cm^2) in the absence or presence of SP203580 for the periods indicated. Expression levels of AhR protein or CYP1A1 protein normalized to those of β-actin protein were standardized to the values obtained at 0 h and shown as means ± SD of four independent experiments in the bar graph. *$P < 0.01$. (*D*) HUVECs were exposed to laminar SS (15 dyne/cm^2) in the absence or presence of U0126 for the periods indicated. Protein levels of AhR, CYP1A1, and β-actin were analysed by western blotting. Expression levels of AhR protein or CYP1A1 protein normalized to those of β-actin protein were standardized to the values obtained at 0 h and shown as means ± SD of four independent experiments in the bar graph.

studies demonstrated that EC turnover and DNA synthesis are increased in areas around branch orifices where ECs are exposed to turbulent blood flow and atherosclerotic change is often initiated.[36,37] Therefore, the anti-proliferative effect of laminar SS may be essential for the maintenance of vascular homeostasis. In the present study, si-AhR recovered DNA synthesis that had been suppressed by SS, and also prevented SS from inducing expression of the Cdk inhibitor $p21^{Cip1}$ and de-phosphorylating pRb (*Figure 6B*). Recent studies suggested that by directly interacting with pRb,[38,39] AhR inhibits the E2F-dependent transcription that initiates G_1/S transition, resulting in inhibition of the cell cycle. Our results strongly agree with these results. TCDD was reported to induce cell cycle arrest in G_1 phase through AhR-mediated induction of the Cdk inhibitor $p27^{Kip1}$ in rat hepatoma cell line.[8] However, we previously showed that SS did not change the expression level of $p27^{Kip1}$ in ECs,[18] and therefore, the action of AhR may differ among cell species and stimulants.

There are several limitations in this study. We used BAECs instead of HUVECs for the promoter analysis because of their higher transfection efficiency. Furthermore, we used the rat CYP1A1 promoter sequence to examine promoter activity. Although rat CYP1A1 promoter had a high homology with human CYP1A1 promoter, the differences between species in response to SS cannot be denied.

Our results suggested that the constitutive activation of AhR and CYP1A1 in response to blood flow is a normal physiological mechanism to protect the vascular wall from toxic stimuli, distinct from the pathological role of these

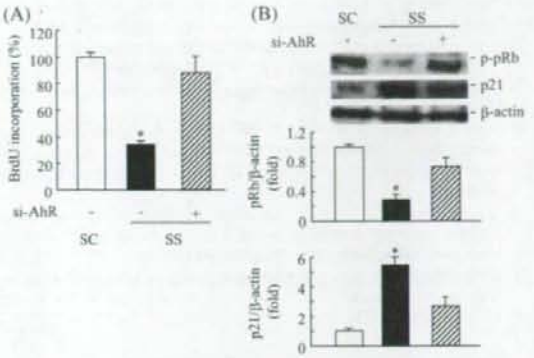

Figure 6 Effects of small interfering RNA for aryl hydrocarbon receptor on shear stress (SS)-induced cell cycle arrest. (*A*) Effects on laminar SS-induced inhibition of DNA synthesis. Once confluent, bovine arterial endothelial cells were immediately exposed to SS (15 dyne/cm^2) for 8 h and thereafter, incubated with BrdU. BrdU incorporation was measured and analysed as described in 'Methods'. The data are presented as values relative to the static control (SC) and shown as means ± SD of four independent experiments in the bar graph. *$P < 0.01$ vs. SC. (*B*) Effects on expressions of p21 and phosphorylated-pRb. Expression levels of proteins normalized to those of β-actin protein were standardized to the values obtained at 0 h and shown as means ± SD of four independent experiments in the bar graph. *$P < 0.01$ vs. SC.

molecules as generators of toxic metabolites. Even though, AhR and CYP1A1 expressed in response to PAHs results in the generation of harmful substances, their initially assumed roles may have been different, since few environmental pollutants such as PAHs existed when these molecules first evolved. Further study is needed to precisely determine the physiological and pathological roles of AhR and CYP1A1 expressed in the vascular wall.

Acknowledgement

We are grateful to Kana Oie for her secretarial assistance.

Conflict of interest: none declared.

Funding

Ministry of Education, Culture, Sports, Science and Technology, Japan [a Grant-in-Aid for Young Scientists (B) No.15790137]; Kyushu University Interdisciplinary Programs in Education and Projects in Research Development.

References

1. Poland A, Knutson JC. 2,3,7,8-tetrachlorodibenzo-p-dioxin and related halogenated aromatic hydrocarbons: examination of the mechanism of toxicity. *Annu Rev Pharmacol Toxicol* 1982;**22**:517–554.
2. Whitlock JP Jr. Genetic and molecular aspects of 2,3,7,8-tetrachlorodibenzo-p-dioxin action. *Annu Rev Pharmacol Toxicol* 1990; **30**:251–277.
3. Mimura J, Fujii-Kuriyama Y. Functional role of AhR in the expression of toxic effects by TCDD. *Biochim Biophys Acta* 2003;**1619**:263–268.
4. Ross JS, Stagliano NE, Donovan MJ, Breitbart RE, Ginsburg GS. Atherosclerosis and cancer: common molecular pathways of disease development and progression. *Ann N Y Acad Sci* 2001;**947**:271–292.
5. Schmidt JV, Bradfield CA. Ah receptor signaling pathways. *Annu Rev Cell Dev Biol* 1996;**12**:55–89.
6. Gonzalez FJ, Fernandez-Salguero P. The aryl hydrocarbon receptor: studies using the AHR-null mice. *Drug Metab Dispos* 1998;**26**:1194–1198.
7. Weiss C, Kolluri SK, Kiefer F, Gottlicher M. Complementation of Ah receptor deficiency in hepatoma cells: negative feedback regulation and cell cycle control by the Ah receptor. *Exp Cell Res* 1996;**226**:154–163.
8. Kolluri SK, Weiss C, Koff A, Gottlicher M. p27(Kip1) induction and inhibition of proliferation by the intracellular Ah receptor in developing thymus and hepatoma cells. *Genes Dev* 1999;**13**:1742–1753.
9. Levine-Fridman A, CHne L, Elferink CJ. Cytochrome P4501A1 promotes G1 phase cell cycle progression by controlling aryl hydrocarbon receptor activity. *Mol Pharmacol* 2004;**65**:461–469.
10. Dey A, Jones JE, Nebert DW. Tissue- and cell type-specific expression of cytochrome P450 1A1 and cytochrome P450 1A2 mRNA in the mouse localized in situ hybridization. *Biochem Pharmacol* 1999;**58**:525–537.
11. Gimbrone MA Jr, Topper JN, Nagel T, Anderson KR, Garcia-Cardena G. Endothelial dysfunction, hemodynamic forces, and atherogenesis. *Ann N Y Acad Sci* 2000;**902**:230–239.
12. Eskin SG, Turner NA, McIntire LV. Endothelial cell cytochrome P450 1A1 and 1B1: up-regulation by shear stress. *Endothelium* 2004;**11**:1–10.
13. McCormick SM, Eskin SG, McIntire LV, Teng CL, Lu CM, Russell CG *et al.* DNA microarray reveals changes in gene expression of shear stressed human umbilical vein endothelial cells. *Proc Natl Acad Sci USA* 2001; **98**:8955–8960.
14. Davies PF. Flow-mediated endothelial mechanotransduction. *Physiol Rev* 1995;**75**:519–560.
15. Traub O, Berk BC. Laminar shear stress: mechanisms by which endothelial cells transduce an atheroprotective force. *Arterioscler ThrombVasc Biol* 1998;**18**:677–685.
16. Dimmeler S, Haendeler J, Rippmann V, Nehls M, Zeiher AM. Shear stress inhibits apoptosis of human endothelial cells. *FEBS Lett* 1996;**399**:71–74.
17. Thum T, Haverich A, Borlak J. Cellular dedifferentiation of endothelium is linked to activation and silencing of certain nuclear transcription factors: implications for endothelial dysfunction and vascular biology. *FASEB J* 2000;**14**:740–751.
18. Akimoto S, Mitsumata M, Sasaguri T, Yoshida Y. Laminar shear stress inhibits vascular endothelial cell proliferation by inducing cyclin-dependent kinase inhibitor p21$^{Sdi1/Cip1/Waf1}$. *Circ Res* 2000;**86**:185–190.
19. Kosaka C, Sasaguri T, Masuda J, Zen K, Shimokado K, Yokota T *et al.* Protein kinase C-mediated inhibition of cyclin A expression in human vascular endothelial cells. *Biochem Biophys Res Commun* 1993;**193**:991–998.
20. Sokabe T, Yamamoto K, Ohura N, Nakatsuka H, Qin K, Obi S *et al.* Differential regulation of urokinase-type plasminogen activator expression by fluid shear stress in human coronary artery endothelial cells. *Am J Physiol Heart Circ Physiol* 2004;**287**:H2027–H2034.
21. Takahashi-Yanaga F, Taba Y, Miwa Y, Kubohara Y, Watanabe Y, Hirata M *et al. Dictyostelium* differentiation-inducing factor-3 activates glycogen synthase kinase-3ß and degrades cyclin D1 in mammalian cells. *J Biol Chem* 2003;**278**:9663–9670.
22. Willett KL, Gardinali PR, Sericano JL, Wade TL, Safe SH. Characterization of the H4IIE rat hepatoma cell bioassay for evaluation of environmental samples containing polynuclear aromatic hydrocarbons (PAHs). *Arch Environ Contam Toxicol* 1997;**32**:442–448.
23. Miyagi M, Miwa Y, Takahashi-Yanaga F, Morimoto S, Sasaguri T. Activator protein-1 mediates shear stress-induced prostaglandin D synthase gene expression in vascular endothelial cells. *Arterioscler Thromb Vasc Biol* 2005;**25**:970–975.
24. Tan Z, Chang X, Puga A, Xia Y. Activation of mitogen-activated protein kinases (MAPKs) by aromatic hydrocarbons: role in the regulation of aryl hydrocarbon receptor (AHR) function. *Biochem Pharmacol* 2002; **64**:771–780.
25. Shibazaki M, Takeuchi T, Ahmed S, Kikuchi H. Suppression by p38 MAP kinase inhibitors (pyridinyl imidazole compounds) of Ah receptor target gene activation by 2,3,7,8-tetrachlorodibenzo-p-dioxin and the possible mechanism. *J Biol Chem* 2004;**279**:3869–3876.
26. Yim S, Oh M, Choi SM, Park H. Inhibition of the MEK-1/p42 MAP kinase reduces aryl hydrocarbon receptor-DNA interactions. *Biochem Biophys Res Commun* 2004;**322**:9–16.
27. Jo H, Sipos K, Go YM, Law R, Rong J, McDonald JM. Differential effect of shear stress on extracellular signal-regulated kinase and N-termial Jun kinase in endothelial cells. *J Biol Chem* 1997;**272**:1395–1401.
28. Pearce MJ, McIntyre TM, Prescott SM, Zimmerman GA, Whatley RE. Shear stress activates cytosolic phospholipase A_2 (cPLA$_2$) and MAP kinase in human endothelial cells. *Biochem Biophys Res Commun* 1996;**218**: 500–504.

29. Tseng H, Peterson TE, Berk BC. Fluid shear stress stimulates mitogen-activated protein kinase in endothelial cells. *Circ Res* 1995;**77**: 869–878.
30. Castro-Rivera E, Wormke M, Safe S. Estrogen and aryl hydrocarbon responsiveness of ECC-1 endometrial cancer cells. *Mol Cell Endocrinol* 1999;**150**:11–21.
31. Pollenz RS, Sattler CA, Poland A. The aryl hydrocarbon receptor and aryl hydrocarbon receptor nuclear translocator protein show distinct subcellular localizations in Hepa 1c1c7 cells by immunofluorescence microscopy. *Mol Pharmacol* 1994;**45**:428–438.
32. Pollenz RS. The aryl-hydrocarbon receptor, but not the aryl-hydrocarbon receptor nuclear translocator protein, is rapidly depleted in hepatic and nonhepatic culture cells exposed to 2,3,7,8-tetrachlorodibenzo-p-dioxin. *Mol Pharmacol* 1996;**49**:391–398.
33. Yim S, Oh M, Choi SM, Park H. Inhibition of the MEK-1/p42 MAP kinase reduces aryl hydrocarbon receptor–DNA interactions. *Biochem Biophys Res Commun* 2004;**322**:9–16.
34. Tan Z, Huang M, Puga A, Xia Y. A critical role for MAP kinases in the control of Ah receptor complex activity. *Toxicol Sci* 2004;**82**:80–87.
35. Caplan BA, Schwartz CJ. Increased endothelial cell turnover in areas of in vivo Evans blue uptake in the pig aorta. *Atherosclerosis* 1973;**17**:401–417.
36. Wright HP. Mitosis patterns in aortic endothelium. *Atherosclerosis* 1972; **15**:93–100.
37. Kunz J, Schreiter B, Schubert B, Voss K, Krieg K. Experimental investigations on the regeneration of aortic endothelial cells: automatic and visual evaluation of autoradiograms [in German]. *Acta Histochem* 1978; **61**:53–63.
38. Ge NL, Elferink CJ. A direct interaction between the aryl hydrocarbon receptor and retinoblastoma protein. Linking dioxin signaling to the cell cycle. *J Biol Chem* 1998;**273**:22708–22713.
39. Elferink CJ, Ge NL, Levine A. Maximal aryl hydrocarbon receptor activity depends on an interaction with the retinoblastoma protein. *Mol Pharmacol* 2001;**59**:664–673.